

We are IntechOpen, the world's leading publisher of Open Access books Built by scientists, for scientists

6,900

Open access books available

186,000

International authors and editors

200M

Downloads

Our authors are among the

154

Countries delivered to

TOP 1%

most cited scientists

12.2%

Contributors from top 500 universities



WEB OF SCIENCE™

Selection of our books indexed in the Book Citation Index
in Web of Science™ Core Collection (BKCI)

Interested in publishing with us?
Contact book.department@intechopen.com

Numbers displayed above are based on latest data collected.
For more information visit www.intechopen.com



Influence of Post-Deposition Thermal Treatment on the Opto-Electronic Properties of Materials for CdTe/CdS Solar Cells

Nicola Armani¹, Samantha Mazzamuto² and Lidice Vaillant-Roca³

¹IMEM-CNR, Parma

²Thifilab, University of Parma, Parma

³Lab. of Semicond. and Solar Cells, Inst. of Sci. and Tech. of Mat.,
Univ. of Havana, La Habana

^{1,2}Italy

³Cuba

1. Introduction

Thin film solar cells based on polycrystalline Cadmium Telluride (CdTe) reached a record efficiencies of 16.5% (Wu et al. 2001a) for laboratory scale device and of 10.9% for terrestrial module (Cunningham, 2000) about ten years ago. CdTe-based modules production companies have already made the transition from pilot scale development to large manufacturing facilities. This success is attributable to the peculiar physical properties of CdTe which make it ideal for converting solar energy into useful electricity at an efficiency level comparable to silicon, but by consuming only about 1% of the semiconductor material required by Si solar cells. Because of the easy up-scaling to an industrial production as well as the low cost achieved in the recent years by the manufacturers, the CdTe technology has carved out a remarkable part of the photovoltaic market. Up to now two companies (Antec Solar and First Solar) have a noticeable production of CdTe based modules, which are assessed as the best efficiency/cost ratio among all the photovoltaic technologies.

Since the record efficiency of such type solar cells is considerably lower than the theoretical limit of 28-30% (Sze, 1981), the performance of the modules, through new advances in fundamental material science and engineering, and device processing can be improved. Further studies are required to reveal the physical processes determining the photoelectric characteristics and the factors limiting the efficiency of the devices.

The turning point for obtaining the aforementioned high efficiency values was the application of a Cl-based thermal treatment to the structures after depositing the CdTe layer (Birkmire & Meyers, 1994; McCandless & Birkmire, 1991). The device performance improvement is due to a combined beneficial effect on the materials properties and on the p-n junction characteristics. CdTe grain size increase (Enriquez & Mathew, 2004; Luschitz et al., 2009), texture properties variations (Moutinho et al., 1998), grain boundary passivation, as well as strain reduction due to S diffusion from CdS to the CdTe layer and recrystallization mechanism (McCandless et al., 1997) are the common observed effects.

In the conventional treatment, based on a solution method, the as-deposited CdTe is coated by a CdCl₂ layer and then annealed in air or inert gas atmosphere at high temperature. Afterwards, an etching is usually made to remove some CdCl₂ residuals and oxides and to leave a Te-rich CdTe surface ready for the back contact deposition. This etching is usually carried out with a Br-methanol solution or by using a mixture of HNO₃ and HPO₃. Alternative methodologies avoiding the use of solutions have been developed: the CdTe films are heated in presence of CdCl₂ vapor or a mixture made by CdCl₂ and Cl₂ vapor, or HCl (Paulson & Dutta 2000). Vapor based treatments reduce processing time since combining the exposure to CdCl₂ and annealing into one step.

All these post-deposition treatments have been demonstrated to strongly affect the morphological, structural and opto-electronic properties of the structures. The changes induced by the chlorine based treatments depend on how the CdTe and CdS were deposited. For example, in CdTe films having an initial sub micrometer grain size, it promotes a recrystallization mechanism, followed by an increase of the grains. This recrystallization process takes place in all CdTe films having specific initial physical properties, and does not depend on the deposition method used to grow the films. Recrystallization together to grain size increase has been observed in CdTe films deposited by Closed Space Sublimation (CSS), Physical Vapor Deposition (PVD) or Radio Frequency Sputtering. The chlorine based treatment may or may not induce recrystallization of the CdTe films, depending on the initial stress state of the material, and the type and conditions of the treatment. For this reason, the recrystallization process wasn't observed in CSS samples which are deposited at higher temperatures and have an initial large grain size, while, for example CdTe films deposited by Sputtering that are characterized by small grains lower than 1 μm in size, an increase up to one order of magnitude was obtained (Moutinho et al., 1998, 1999). The driving force for the recrystallization process is the lattice-strain energy at the times and temperatures used in the treatment.

Changes in structural properties and preferred orientation are also observed. The untreated CdTe material usually grows in the cubic zincblende structure, with a preferential orientation along the (111) direction. Depending on the deposition method, these texture properties can be lost, in place of a completely disoriented material. The Cl-based annealing induces a loss of the preferential orientation as demonstrated by literature X-Ray Diffraction (XRD) works explaining in terms of σ value calculation (Moutinho et al. 1998, 1999). However, this treatment is important even in films that do not recrystallize because it decreases the density of deep levels inside the bandgap and changes the defect structure, resulting in better devices.

Maybe the crucial effect of the treatment is related to the p-n junction characteristics. This treatment promotes interdiffusion between CdTe and CdS, resulting in the formation of CdTeS alloys at the CdTe–CdS interface. The CdTe_{1-x}S_x and CdS_{1-y}Te_y alloys form via diffusion across the interface during CdTe deposition and post-deposition treatments and affect photocurrent and junction behavior (McCandless & Sites, 2003).

Formation of the CdS_{1-y}Te_y alloy on the S-rich side of the junction reduces the band gap and increases absorption which reduces photocurrent in the 500–600 nm range. Formation of the CdTe_{1-x}S_x alloy on the Te-rich side of the junction reduces the absorber layer bandgap, due to the relatively large optical bowing parameter of the CdTe–CdS alloy system.

Despite the promising results, the transfer to an industrial production of the commonly adopted CdCl₂ based annealing may increase the number of process steps and consequently the device final cost (Ferekides et al., 2000). Since CdCl₂ has a quite low evaporation

temperature (about 500°C in air), it cannot be stored in a large quantity, since it is dangerous because it can release Cd in the environment in case of fire. Secondly, CdCl₂ is soluble in water and, as a consequence, severe security measures must be taken to preserve environmental pollution and health damage. Another drawback is related to the use of chemical etchings, such as HNO₃ and HPO₃ or Br-Methanol solution, implying that a proper disposal of the used reagents has to be adopted since the workers safety in the factory must be guaranteed. In order to overcome the aforementioned drawbacks, we substituted the CdCl₂ based process with an alternative, completely dry CdTe post-deposition thermal treatment, based on the use of a mixture of Ar and a gas belonging to the Freon family and containing chlorine, such as difluorochloromethane (HCF₂Cl) (Bosio et al., 2006, Romeo N. et al., 2005). This gas is stable and inert at room temperature and it has not any toxic action. Moreover, the post-treatment chemical etching procedures have been eliminated by substituting them with a simple vacuum annealing.

The only drawback in using a Freon gas could be that it is an ozone depleting agent, but, in an industrial production, it can be completely recovered and reused in a closed loop. In this paper, it will be demonstrated how the CdTe treatment in a Freon atmosphere works as well as the treatment carried out in presence of CdCl₂.

This method was successfully applied to Closed Space Sublimation (CSS) CdS/CdTe solar cells, by obtaining high-efficiency up to 15% devices (Romeo N. et al., 2007). This original approach may produce modifications on the material properties, different than the usual CdCl₂-based annealing. For this reason, in this work, the efforts are focused on the investigation of the peculiar effects of the treatment conditions on the morphology, structural and luminescence properties of CdTe thin films deposited by CSS on Soda-Lime glass/TCO/CdS. All the samples were deposited by keeping unmodified the growth parameters (temperatures and layer thicknesses), in order to submit as identical as possible materials to the annealing. Only the HCF₂Cl partial pressure and the Ar total pressure in the annealing chamber have been varied.

The aim of the present work is to correlate the effect of this new, all dry post-deposition treatment, on the sub-micrometric electro-optical properties of the CSS deposited CdTe films, with the effect on the device performances. Large area SEM-cathodoluminescence (CL) analyses have allowed us to observe an increase of the overall luminescence efficiency and in particular a clear correlation between the defects related CL band and the HCF₂Cl partial pressure in the annealing atmosphere. By the high spatial (lateral as well as in-depth) resolution of CL, a sub-micrometric investigation of the single grain radiative recombination activity and of the segregation of the atomic species, coming from the Freon gas, into grain boundary has been performed.

The HCF₂Cl partial pressure has been changed from 20 to 50 mbar, in order to discriminate the Freon gas effect from the others annealing parameters. A clear correlation between the CL band intensities and the HCF₂Cl partial pressure has been found and a dependence on the lateral luminescence distribution has been observed.

The results obtained from the material analyses have been correlated to the performances of the solar cells processed starting from the glass/ITO/ZnO/CdS/CdTe structures studied. Electrical measurements in dark and under illumination were carried out, in order to determine the characteristic photovoltaic parameters of the cell and to investigate the transport processes that take place at the junction. In particular the device short circuit current density (J_{sc}), open circuit voltage (V_{oc}) fill factor (ff) and efficiency (η) have been measured as a function of the HCF₂Cl partial pressure. The most efficient device obtained by

this procedure, corresponding to 40 mbar HCF_2Cl partial pressure in the 400mbar Ar total pressure, has $\eta=14.8\%$, $J_{\text{SC}}=26.2\text{mA}/\text{cm}^2$, $V_{\text{OC}} = 820\text{mV}$ and $\text{ff}=0.69$.

The solar cells were then submitted to an etching procedure in a Br-methanol mixture at 10% to eliminate the back contacts and part of the CdTe material in some portion of the specimens. On the beveled surface, CL analyses have been performed again in order to extract information as close as possible to the CdTe/CdS interface and to compare the results to the depth-dependent CL analyses.

Finally, a model of the electronic levels present in the CdTe bandgap before and after the HCF_2Cl treatment has been proposed as well as a model of the interface region modifications due to the annealing.

2. Materials growth and devices preparation

CdTe is a II-VI semiconductor with a direct energy-gap of 1.45eV at room temperature that, combined with the very high absorption coefficient, $10^4\text{-}10^5\text{ cm}^{-1}$ in the visible light range, makes it one of the ideal materials for photovoltaic conversion, because a layer thickness of a few micrometers is sufficient to absorb 90% of incident photons. For thin film solar cells is required a p-type material, which is part of the p-CdTe/n-CdS heterojunction. The electrical properties control was easily developed for single-crystal CdTe, grown from the melt or vapor, at high temperature (above 1000°C), by introducing doping elements during growth. On the contrary, in polycrystalline CdTe, where grain boundaries are present, all metallic dopants tend to diffuse along the grain boundaries, making the doping unable to modify the electrical properties and producing shunts in the device.

CdTe solar cell is composed by four parts (Fig. 1) deposited on a substrate like Soda-Lime Glass (SLG):

1. The *Front Contact* is composed by a Transparent Conducting Oxide (TCO) that is a doped metallic oxide like $\text{In}_2\text{O}_3:\text{Sn}$ (ITO)(Romeo N. et al., 2010) , $\text{ZnO}:\text{Al}$ (AZO)(Perrenoud et al., 2011), CdSnO_4 (CTO)(Wu, 2004), $\text{SnO}_2:\text{F}$ (FTO) (Ferekides et al., 2000), etc.; and a very thin layer of a resistive metal oxide like SnO_2 (Ferekides et al., 2000), ZnO (Perrenoud et al., 2011; Romeo N. et al. 2010), Zn_2SnO_4 (Wu et al. 2001b). The role of the latter film is to hinder the diffusion of contaminant species from TCO and SLG toward the upper layers of the cell such as the window layer (CdS) or the absorber one (CdTe). Moreover it separates TCO and CdS in order to limit the effects of pinholes that could be present in CdS film.
In our work, TCO is made by 400nm thick ITO film and 300nm thick ZnO both of them deposited by sputtering. ITO showed a sheet resistance of about $5\Omega/\text{cm}^2$, while the resistivity of ZnO was on the order of $10^3\Omega\text{ cm}$.
2. The *Window Layer* is usually an n-type semiconductor; Cadmium Sulphide (CdS) is the most suitable material for CdTe-based solar cells, thanks to its large bandgap (2.4eV at room temperature) and because it grows with n-type conductivity without the introduction of any dopants. Here, CdS film was deposited by reactive RF sputtering in presence of Ar+10% CHF_3 flux. Its nominal thickness was 80nm.
3. The *Absorber Layer* is a 6-10 μm thick film. The deposition techniques and the treatment on CdTe will be explained deeply later.
4. The *Back Contact* is composed by a buffer layer and a Mo or W film. The utility of the buffer layer is to form a low resistive and ohmic contact on CdTe.

The cell is completed by a scribing made on the edge of all the cells in order to electrically separate the front contact from the back one.

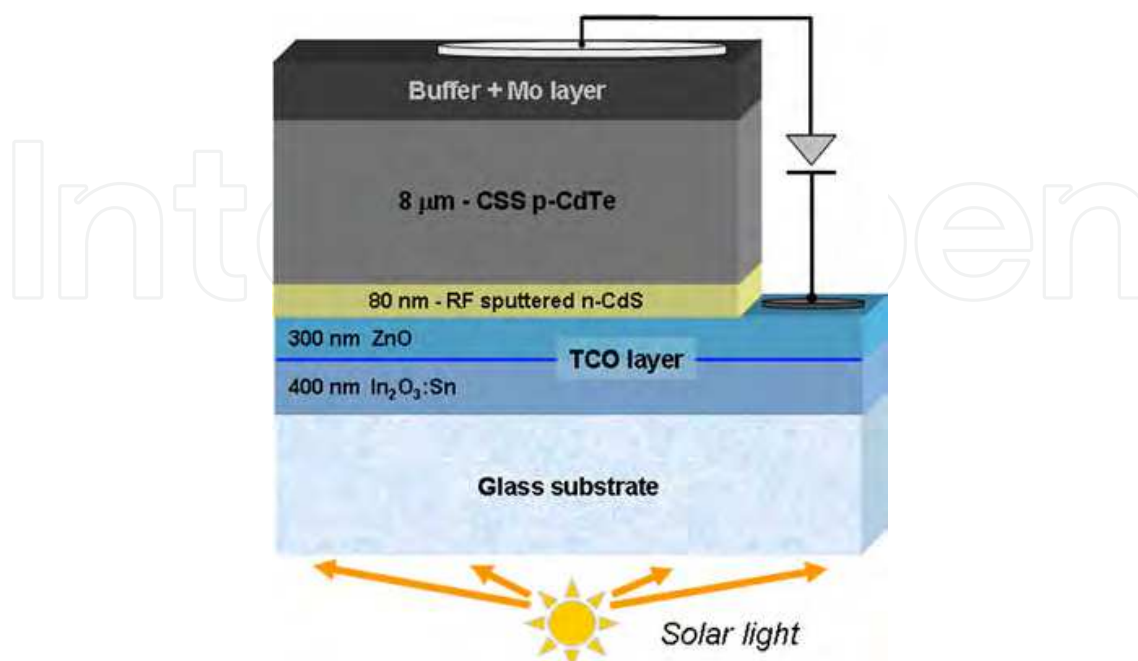


Fig. 1. Schematic representation of the CdS/CdTe solar cell heterostructure. The layers succession and thicknesses are the ones used in the present work.

2.1 CSS Growth of CdTe layers

CdTe thin films have been deposited by several deposition techniques such as High Vacuum Evaporation (HVE)(Romeo A. et al., 2000), Electro-Deposition (ED)(Josell et al., 2009; Kosyachenko et al., 2006; Levy-Clement, 2008; Lincot, 2005), Chemical Vapour Deposition (CVD)(Yi & Liou, 1995), Metal-Organic Chemical Vapor Deposition (MOCVD)(Barrioz, 2010; Hartley, 2001; Zoppi, 2006), Spray Pyrolysis (Schultz et al., 1997), Screen Printing (Yoshida, 1992 & 1995) Sputtering (Compaan et al., 1993; Hernández-Contreras et al., 2002; Plotnikov et al., 2011) and Close Spaced Sublimation (CSS)(Chu et al., 1991; Romeo N. et al., 2004; Wu, 2004).

Among these techniques, CdTe deposited by CSS allowed to obtain best results for solar cells (world record photovoltaic solar energy conversion ~16.5%; Wu, 2004).

CSS is a physical technique based on a high temperature process. The apparatus is showed in Fig. 2 and it is composed by a vacuum chamber inside which the substrate and the source are placed at a distance of few millimeters (2-7mm). The difference in temperature between the substrate and the source is kept around 50-150°C. Deposition takes place in presence of an inert gas (Ar) or a reactive one (O₂, etc.) with a total pressure of about 1-100mbar. The gas creates a counter-pressure which reduces re-evaporation from the substrate and forces the atoms from the source to be scattered many times by the gas atoms before arriving to the substrate, so that the material to be deposited acts like it has a higher dissociation temperature and higher temperature respect to sublimation under vacuum are necessary.

CSS allows to obtain CdTe film with a very high crystalline quality and grains of about one order of magnitude larger (~10μm) than films deposited by other deposition techniques (Sputtering, HVE, etc.) and, for this reason, with a low lattice defect density (Romeo A. et al., 2009).



Fig. 2. Picture of the CSS setup used for growing the CdTe films studied (left); Detail of the growth region of the CSS chamber (right).

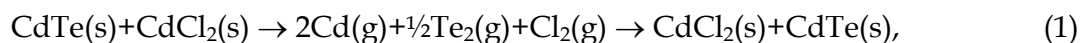
In our work, CdTe was deposited in 1mbar Ar atmosphere, keeping the substrate and source temperatures at 500°C and 600°C respectively. The CdTe thickness was 6-8 μm .

The high substrate temperature ($\sim 500^\circ\text{C}$) favors the formation of a mixed compound $\text{CdS}_x\text{Te}_{1-x}$ at the interface between CdS and CdTe directly during CdTe deposition, as shown in the phase diagram (Lane et al., 2000). The mixed compound formation, by means of S diffusion toward CdTe and Te diffusion toward CdS, is advantageous in order to get high efficiency CdS/CdTe solar cells. In fact, its formation is required in order to minimize defect density at the interface acting as traps for majority carriers crossing the junction, caused by the lattice mismatch between CdS and CdTe that is about 10%.

2.2 HCF_2Cl post-deposition thermal treatment

The Cl-treatment on CdTe surface is a key point in order to rise the photocurrent and so the efficiency of the solar cell.

During Cl-treatment CdTe goes in vapor phase as explained by the following reaction (McCandless, 2001):



where s is the solid phase and g is the vapor phase.

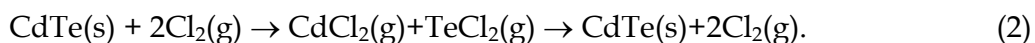
After the treatment small grains disappear from CdTe surface and at the same time an increase in grain dimensions and an improvement in crystal organization can be observed. Also an improvement, in the crystal organization of the mixed compound $\text{CdS}_x\text{Te}_{1-x}$, at the junction, formed during CdTe deposition, can be observed.

Usually Cl-treatment is carried out by depositing on CdTe surface a CdCl_2 (thickness more than 100nm) film by evaporation (Potter et al., 2000; Romeo A. et al. 2000; Romeo N. et al. 1999) or by dipping CdTe in a CdCl_2 -methanol solution (Cruz et al., 1999), then an annealing at $\sim 380\text{--}420^\circ\text{C}$ in an Ar atmosphere or in air is required and finally, an etching in Br-methanol or an annealing in vacuum is carried out in order to remove CdCl_2 residuals on CdTe surface. The main drawback of this treatment is that CdCl_2 , being very hygroscopic, could be dangerous either for people and for the environment since it can release free Cd.

We have proposed a new treatment by substituting CdCl_2 , or CdCl_2 -methanol solution, and the following etching with a treatment at 400°C in a controlled atmosphere containing a gas belonging to the Freon® family which can free Cl at high temperature. This gas is very

stable and inert at the room temperature; moreover, in the case of an industrial production, it can be re-used in a closed loop without releasing it in atmosphere.

We suppose that the following reaction happens at 400°C during the treatment (Romeo N. et al., 2006):



After that, an annealing is carried out at the same temperature of the treatment for few minutes in vacuum (10^{-5} mbar) in order to let CdCl_2 residuals re-evaporate and to obtain a clean CdTe surface ready for the back contact deposition.

In this work, the TCO/CdS/CdTe system is placed in an evacuable quartz ampoule. Before each run, the ampoule is evacuated with a turbo-molecular pump up to 10^{-6} mbar. As a source of Cl_2 , a mixture of $\text{Ar} + \text{HCF}_2\text{Cl}$ is used. The samples were prepared by changing the HCF_2Cl partial pressure. The first one was an untreated sample, while the other four ones were made by choosing four values of HCF_2Cl partial pressure that are 20, 30, 40, and 50 mbar and keeping the total pressure ($\text{Ar} + \text{HCF}_2\text{Cl}$) at 400 mbar. An additional specimen, annealed at 30 mbar HCF_2Cl partial pressure, but with a larger total $\text{Ar} + \text{HCF}_2\text{Cl}$ pressure of 800 mbar, has been prepared, in order to study the effect of the total pressure on the recrystallization mechanisms. The Ar and the HCF_2Cl partial pressures were independently measured by two different capacitance vacuum gauges and monitored by a Varian Multi-Gauge. The quartz tube is put into an oven where a thermocouple is installed in order to control the furnace temperature, which is set at 400°C. The annealing time is 10 min for all samples studied in this work. After the treatment, a vacuum for about 10 min, keeping the temperature at 400°C, was made in order to remove some CdCl_2 residuals from the CdTe surface.

2.3 Back contact deposition and device processing

The cell is completed by back contact deposition. The formation of a ohmic and stable back contact with CdTe has always been one of the most critical points in order to obtain high efficiency CdS/CdTe solar cells. Normally, CdTe is etched in order to get a Tellurium rich surface. After that, a Cu film (~2 nm thick) is deposited in order to form a Cu_xTe compound that is a good non-rectifying contact for CdTe. This procedure has two disadvantages: chemical etching is not convenient because it is not scalable to an industrial level and it is polluting and the Cu thickness is too small to be controlled. In fact, if a thicker Cu film is deposited it could happen that Cu is free from the Cu_xTe formation and it could cause short circuits in the cell because it can segregate in grain boundaries.

In our work, back contact is composed by the deposition in sequence of three films. A 150-200 nm thick As_2Te_3 film and a 10-20 nm thick Cu film are deposited in sequence on CdTe surface by RF sputtering in Ar flux. When the deposition temperature of Cu is about 150-200°C, a substitution reaction occurs between Cu and As_2Te_3 whose final product material is Cu_xTe , mainly $\text{Cu}_{1.4}\text{Te}$ is the most stable compound (Romeo N. et al, 2006; Wu et al. 2006; Zhou, 2007). Finally, a Mo layer is deposited on top of the cell by sputtering.

2.4 Etching procedures by a Br – methanol mixture

The possibility to perform depth-dependent CL analyses, by increasing the energy of the incident electrons of the SEM, allows us to correlate the results obtained on the isolated CdTe to an analysis of the electro-optical properties close to the CdTe/CdS interface region of a complete solar cell. To do this, it is necessary to overcome the problem that summing

the back contact to the CdTe thickness, the main junction is situated around 10 μ m below the specimen surface. This thickness is 2 times higher than the maximum distance that the most energetic electrons in our SEM (40keV) penetrate in CdTe. In addition, it has to take into account that the back contact completely absorbs the light coming from the CdTe film, impeding any CL analyses.

In this work, a solution to this experimental difficulty has been proposed by etching the material to completely eliminate the back contact and the excess CdTe in some portion of the cells. In order to prevent the introduction of superficial defects that would affect the CL reliability, polishing methods were avoided. On the other hand, standard nitric-phosphoric acid chemical etching widely performed before metallization to improve contact formation, shows a strong preferential chemical reaction over the grain boundaries (Bätzner et al. 2001; Xiaonan et al. 1999). For these reasons, a Br-methanol mixture at 10% has been used, expecting to obtain a less selective interaction of the etching solution between the grains and its boundaries.

3. Experimental and set-up description

The methodological approach used in this work was based on the correlation between the study of HCF₂Cl treatment effect on CdTe material properties and the characterization of the photovoltaic cells parameters. There are not many works in literature that correlate the effects of CdTe post-deposition treatment and the relative changes in the electro-optical properties of CdTe with the performance of the photovoltaic device. Only recent studies (Consonni et al. 2006) on the behavior of Cl inside polycrystalline CdTe gave major results about the compensation mechanisms and the formation of complexes between native point defects (NPD) and impurities, already well established in the case of high quality single crystal CdTe (Stadler et al., 1995). The influence of post-deposition treatment on the CdTe/CdS interface region was crucial in the improvement of the device performances. The in-depth CdTe thin film properties, obtained by CL analyses, are then compared to results obtained on etched CdTe samples, treated in the same HCF₂Cl conditions. This allows us to verify the reliability of CL depth-resolution studies on polycrystalline materials and the effect of HCF₂Cl thermal treatment on the bulk CdTe properties approaching the CdTe/CdS interface.

3.1 Cathodoluminescence spectroscopy and mapping

CL is a powerful technique for studying the optical properties of semiconductors. It is based on the detection of the light emitted from a material excited by a highly energetic electron beam. The high-energy electron beam (acceleration voltage between 1-40kV), impinging on the sample surface, creates a large number of electron hole (e-h) pairs. After a thermalization process, the carriers reach the edges of the respective bands, conduction band (CB) in the case of electrons, valence band (VB) in the case of holes, and then diffuse. From the band edges, the electrons and holes can recombine, in the case of radiative recombination, the photons produce the CL signal. A more detailed description of the principles of the CL theory, in particular the fundamental of the generation and recombination mechanisms of the carriers can be found in the works of B. Yacobi and D. Holt (Yacobi & Holt, 1990) and references therein included.

CL is contemporary a microscopic and spectroscopic methodology with high spatial, lateral as well as in-depth, resolution and good spectral resolution when luminescence is detected

at low temperature. These advantages are due to the use of a focused electron beam of a SEM as excitation source. In addition, this technique allows the contemporary acquisition of spectra of the intensity of the light collected as a function of wavelength and images (mono- and pan-chromatic) of the distribution of the light. The results can be acquired from regions of different area, from 1 to several hundreds of μm^2 , depending on the magnification of the SEM and on the dimensions of the parabolic mirror used as light collector.

The lateral resolution in CL imaging can be roughly defined as the minimum detectable distance between two regions presenting different CL intensity. In the SEM-CL, the spatial imaging resolution depends mainly on the size of the recombination volume (generation volume broadened for the diffusion length) of e-h pairs inside the material, entailing also a dependence on the diffusion length (L) of generated carriers. A typical value of the lateral resolution of about 200nm can be reached as a lower limit in suitable working conditions for instance on III-V semiconducting quantum confined heterostructures (Merano et al., 2006).

The in-depth analysis is a CL peculiarity which allows us to investigate the samples at different depths by changing the energy of the primary electrons. The generation, as well as the recombination volume, increases in all the three dimensions by increasing the acceleration voltage. The depth, at which the maximum CL signal is created, increases also by increasing the beam energy (E_b). By this method, it is possible to investigate crystals or thick layers inhomogeneities along the growth direction. The large grain size of the CSS deposited CdTe, higher than 1 μm , allowed us to directly investigate the grain and the grain boundary recombination properties. This possibility is very useful to study a possible gettering mechanism or a passivation effect of the grain boundaries due to the annealing.

The post-deposition thermal treatment has an effect on the CdTe surface as well as on the bulk material, reasonably as far as the CdTe/CdS interface. For this reason, a complete characterization of the CdTe electro-optical properties and of the p-n junction recombination mechanisms, by using a bulk sensitive experimental technique, is necessary. The penetration depth of 200-300nm of the laser radiation used for PL analyses is a disadvantage that could be overcome by using the high energy electrons of an SEM for exciting CL. In addition, the possibility of increasing the CL generation/recombination volume by increasing the electron beam energy allows us a depth-dependent analysis. The CL analysis of 6-8 μm thick CdTe thin films, as the active layers used in the fabrication of solar cells, has particular advantages: the maximum penetration depth of the exciting electrons of the SEM beam can reach 4.8 μm by using 36 keV energy. This depth is higher than the few hundreds of nanometers probed by the commonly used Ar laser (514 nm) to excite PL. It is actually possible to perform an investigation of the CdTe bulk properties by CL in place of a near-surface PL analyses. The in-depth information, that is not available with other micro- and nano-scale optical techniques, is particularly useful for example in the characterization of heterostructures, doping profile, study of extended defects along the growth direction.

However, it is important to remark that the fundamental differences between CL and PL are the amount of e-h pairs generated and the dimensions and shape of the generation volumes. In the case of laser generation, each photon creates a single e-h pair whereas a high energetic electron can generate thousands of e-h pairs. With such a large number of e-h pairs generated, the excitation of all the radiative recombination channels inside the materials is possible.

The instrument used to collect the experimental data reviewed in this work is a Cambridge 360 Stereoscan SEM with a tungsten filament (resulting beam size on the sample surface

typically ranging between a few microns and a few tens of nanometers), equipped with a Gatan MonoCL2 system (Fig. 3). The spectra, as well the panchromatic and monochromatic images, have been acquired using a dispersion system equipped with three diffraction gratings and a system of a Hamamatsu multi-alkali photomultiplier and a couple of liquid nitrogen cooled (Ge and InGaAs) solid state detectors. This experimental set up provides a spectral resolution of 2Å and a detectable 250-2200nm (0.6–4.9eV) wavelength range. By this configuration it is possible to cover a large part of the luminescence emissions of the III-V and II-VI compound semiconductors. In particular, all the possible transitions in CdTe can be detected: from the excitonic lines (around 1.59eV) down to the emissions involving mid-gap levels (0.8-0.9eV). Additionally, it is possible to change the temperature of the samples in the range 5-300K by a temperature controller interlocked with the sample-holder, thanks to a refrigerating system operating with liquid Nitrogen and liquid Helium.

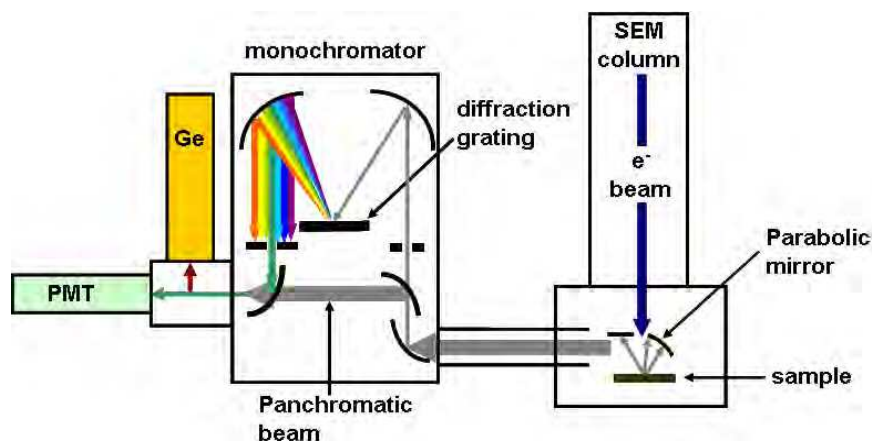


Fig. 3. Schematic representation, not in scale, of the CL experimental setup used in this work.

3.2 X-Ray diffraction

The setup used for acquiring XRD profiles was an X-Ray Diffractometer Thermo arl X'tra, vertical goniometer, theta-theta, operating in an angular range between -8° and 160°, equipped with an X-ray tube, Cu K-alpha and a solid state Si:Li detector. The angular range chosen, between 15° and 80°, assured the detection of all the contributions from the main Bragg diffractions of CdTe: (111), (220), (311), (400), (331), (422), (511).

3.3 Electrical characterization

Light J-V measurements were performed by an Oriel Corporation Solar Cells Test System model 81160, in order to measure the photovoltaic parameters such as the short-circuit current density (J_{sc}), open circuit voltage (V_{oc}), fill factor (ff) and conversion efficiency (η) of the solar cells.

Dark measurements were carried out by a Keithley 236 source system in order to measure the diode quality factor (A) of the cells as a function of the HCF_2Cl partial pressure during the CdTe treatment. A can be calculated from the diode equation in the dark:

$$A = \frac{qV}{kT} \cdot \frac{1}{\ln\left(\frac{J}{J_0} + 1\right)} \quad (3)$$

The measure of A gave some information about the transport mechanism at the junction. If the predominant transport mechanism at the junction is the diffusion then $A \approx 1$, while if the predominant mechanism is the recombination, the value of A increased and approached to 2. The dark conductivity as a function of the temperature (84-300K) and the activation energy were performed by using a Keithley 236 source measure unit. The temperature was set by a system DL4600 Bio-Rad Microscience Division. The samples, used for this measurement, were composed by 300nm thick ZnO, 7 μ m thick CdTe and the back contact. The first sample was a not treated one, while the other two samples were made by treating CdTe with respectively 30 and 40mbar HCF₂Cl partial pressure at 400°C for 10 minutes. The total pressure (Ar+Freon®) was set at 400mbar for all the two samples.

4. Results and discussion

All the CdTe thin films were deposited on SLG/ZnO substrate by CSS; the layer thickness was about 8 μ m. Complete solar cells have been realized by depositing ZnO, CdS and CdTe in the identical conditions and by adding the back contact, as described in paragraphs 2.1 and 2.3. The CdTe films as well as the complete devices were annealed in Ar+HCF₂Cl atmosphere (see for details paragraph 2.2), by increasing the HCF₂Cl partial pressure from 20mbar to 50mbar and keeping the temperature at 400°C for all samples. The annealing conditions used have been summarized in table 1.

Sample	HCF ₂ Cl partial pressure (mbar)	Ar+HCF ₂ Cl total pressure (mbar)	Annealing time (mins)
UT	-	-	-
F20	20	400	10
F30L	30	400	10
F30H	30	800	5
F40	40	400	10
F50	50	400	10

Table 1. Summary of the annealing conditions used to treat the samples studied in this work

4.1 Influence of annealing on the CdTe material properties

The XRD profiles of all the CdTe films were acquired in the angular range 5°<2 θ <80°, from this analysis can be deduced that the films have a zinc-blend structure with a preferential orientation along the (111) direction. In all the XRD patterns the peaks related to (220), (311), (400), (331), (422) and (511) reflections are also visible. In addition a peak at 22.77° attributed to the Te₂O₅ oxide and a peak at 34.34° related to the ZnO (002) reflection are detected. In Fig. 4, only the most representative XRD profiles of the untreated CdTe and of the samples annealed with 40 mbar HCF₂Cl partial pressure were shown.

The preferential orientation of each film is analyzed by using the texture coefficient C_{hkl} , calculated by means of the following formula (Barret & Massalski 1980):

$$C_{hkl} = \frac{I_{hkl}/I_{hkl}^0}{\frac{1}{N} \sum_N I_{hkl}/I_{hkl}^0}, \tag{4}$$

where I_{hkl} is the detected intensity of a generic peak in the XRD spectra, I_{hkl}^0 is the intensity of the corresponding peak for a completely randomly oriented CdTe powder (values taken from the JCPDS) and N the number of reflections considered in the calculation. C_{hkl} values above the unity represented a preferential orientation along the crystallographic direction indicated by the hkl indices. The texture coefficients C_{111} , calculated by the formula Nr 4 for all the samples, are summarized in table 2, together with the CL intensity ratios. A better comprehension of the orientation of each thin film as a whole can be obtained by the standard deviation σ of the C_{hkl} coefficients. Each value has been calculated by the following formula:

$$\sigma = \sqrt{\frac{\sum_N (C_{hkl} - 1)^2}{N}} \quad (5)$$

A complete randomly oriented film is expected to have a σ value as close as possible to 0. The untreated CdTe thin film shows the highest preferential orientation along the (111) direction with a texture coefficient $C_{111}=2.02$. The effect of HCF_2Cl treatment is highlighted by a decrease of the (111) related intensity and by an increase of the relative intensities of the additional reflections (220), (311), (400), (331), (422) and (511), detected. The calculated σ value for the untreated CdTe is also the highest one ($\sigma=0.52$) demonstrating the oriented status of that film. This behavior is evidenced in Fig. 5, in which the calculated peak intensity ratios between each (220), (311), (400), (331), (422) and (511) additional reflection and the (111) one are plotted.

The combined effect of HCF_2Cl partial pressure and the total gas pressure, in the annealing chamber, could be also evidenced by comparing the C_{111} and σ values of the CdTe films treated by 30mbar HCF_2Cl , but higher total pressure (800mbar), sample F30H in table 2. Its values were higher than the CdTe treated with the same partial pressure and lower total pressure (sample F30L in table 1), but similar to the untreated CdTe.

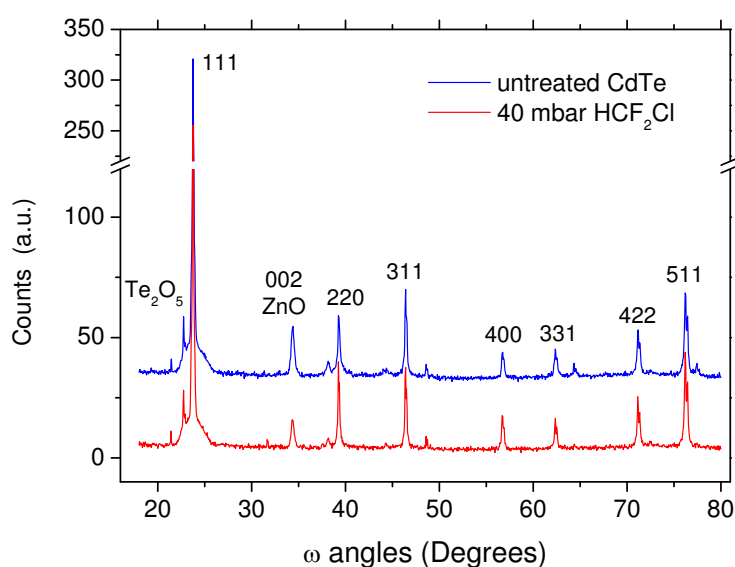


Fig. 4. XRD profiles of the untreated CdTe thin film compared to the sample annealed with 400 mbar Ar+Freon total pressure in the annealing chamber and 40mbar HCF_2Cl partial pressure.

Sample	XRD results		Morphology	1.4 eV/NBE CL intensity	
	C ₁₁₁ texture coefficient	σ	Average grain size (μm)	12 keV	25 keV
UT	2,02	0,52	11.7	0.9	0.72
F30L	1,12	0,29		2.3	3.39
F30H	1,7	0,42	10.8		10.75
F40	1,15	0,31	11.2	14.48	15.47
F50	0,56	0,36		14.74	19.97

Table 2. Summary of the results obtained by processing the XRD profiles, CL spectra and SEM images.

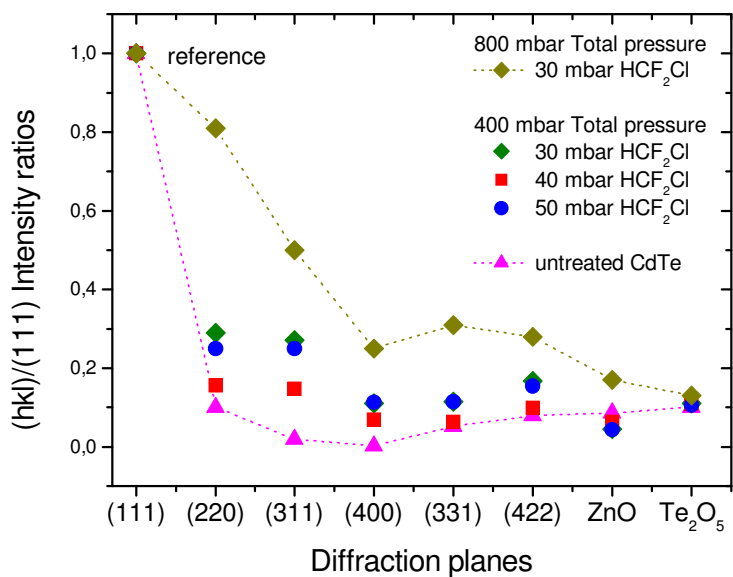


Fig. 5. Plot of intensity ratios among each diffraction (220), (311), (400), (331), (422) and (511) and the (111) one for all the studied CdTe thin films

The loss of preferential orientation due to HCF₂Cl annealing results in a slight modification of the CdTe morphology after the thermal treatment. The untreated CdTe films showed already large grains, as visible in the SEM image of Fig. 6 a. The average grain size obtained by processing the images was 11.7μm and the largest grains reached 20.4μm. The material treated with 40mbar HCF₂Cl partial pressure showed grains with dimensions similar (avg = 11.2μm) to those of the untreated one (Fig. 6 b). The observed average size confirmed that CSS grown CdTe did not show grain size increase after annealing in presence of chlorine as already described in the literature by several authors (Moutinho et al. 1998). Grain dimensions distribution extracted from the SEM images has been represented in histograms showed in Fig. 7 a and b. It could be observed that the small grains density in the HCF₂Cl treated material was reduced, producing a thinner distribution of the histogram columns.

On the contrary, all the Freon treated CdTe showed a remarkable grain shape variation with respect to the untreated sample where most of the grains appeared as tetragonal pyramids with the vertex aligned on the growth direction (Fig. 8 a). This shape justified their high preferential orientation along the (111) direction. This grain shape appeared clearly modified in the HCF₂Cl annealed films. They were more rounded and the pyramids seem to

be made up by a superposition of “terraces” (Fig. 6 b). This morphology change could be correlated to the C_{111} texture coefficient decrease. Two possible mechanisms related to the HCF_2Cl annealing could be invoked: a re-crystallization effect or an “etching-like” erosion of the grain surface. The unmodified grain size and the appearance of the terraces seem to indicate that the latter phenomenon occurred during the Freon treatment.

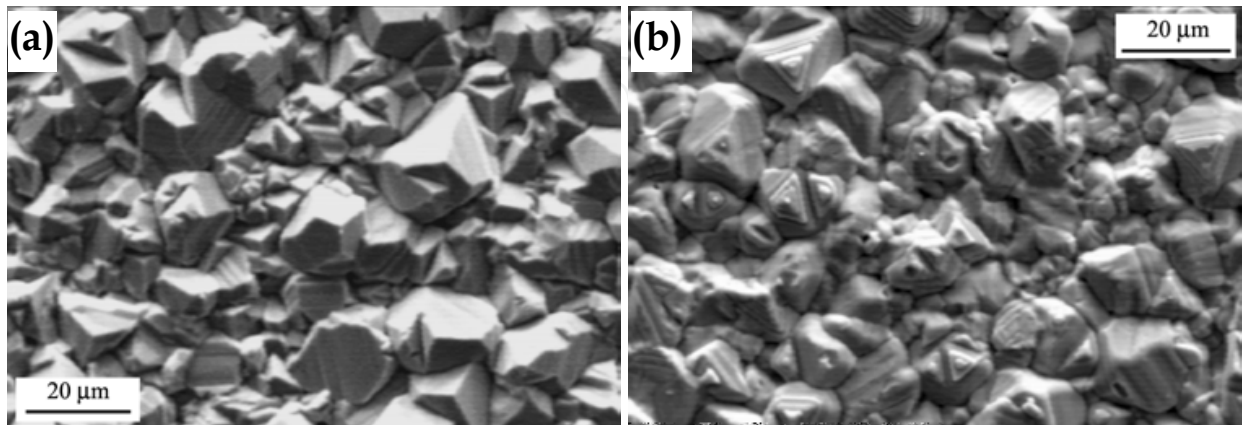


Fig. 6. SEM image of the polycrystalline CdTe surface morphology: a) untreated film; b) annealed with 40mbar HCF_2Cl

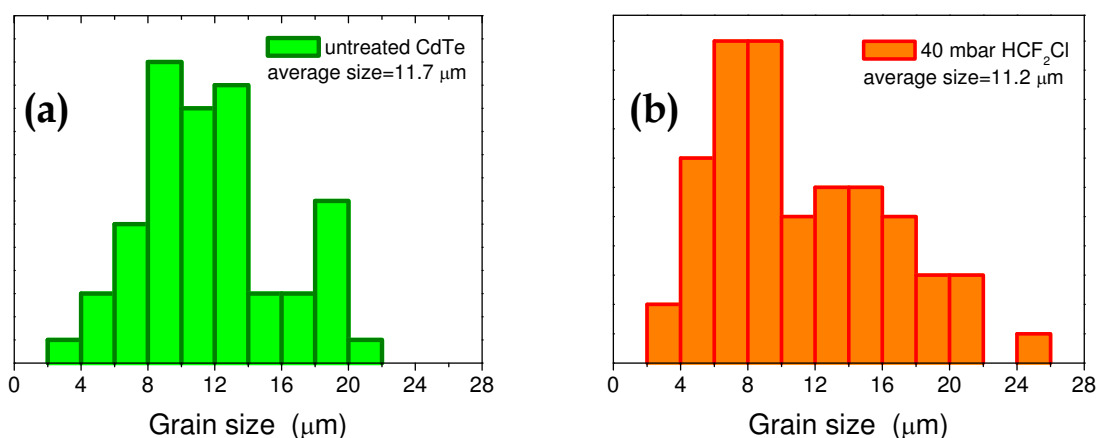


Fig. 7. Histograms of the grain size as obtained from the SEM images: a) untreated CdTe; b) CdTe annealed by 40mbar HCF_2Cl partial pressure.

The effect of thermal treatment on the CdTe bulk electro-optical properties has been studied by acquiring CL spectra at electron beam energy (E_B) of 25keV, corresponding to a maximum penetration depth of about 2.5μm. The CL generation volume dimensions were calculated by means of a numerical approach based on random walk Monte Carlo simulation developed in our laboratory (Grillo et al. 2003). The low temperature (77 K) spectrum of a 240x180 μm² region of the untreated CdTe showed the clear near bend edge (NBE) emission centered at 1.57eV. The temperature is too high to discriminate the acceptor from the donor bound excitonic line, we supposed they were superimposed underneath the NBE band. In addition to the NBE emission, two weak bands, centered at 1.47eV and 1.35eV respectively, were also detected. The 1.35eV and 1.47eV CL peaks were visible only in the untreated CdTe and their origin was not related to the HCF_2Cl treatment. The 1.35eV

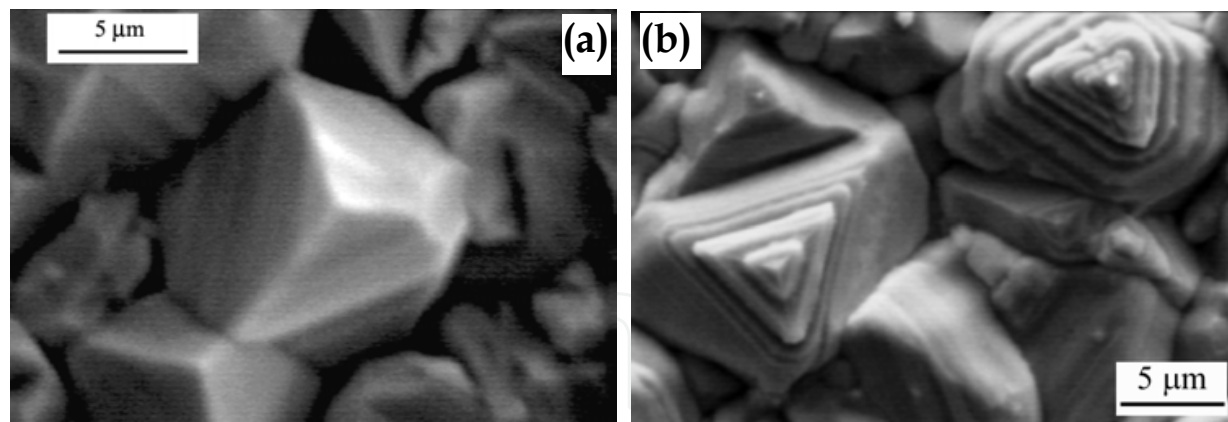


Fig. 8. a) SEM image of a typical pyramidal grain oriented along the (111) growth direction of the untreated film; b) SEM image showing pyramidal grains with terraces of the CdTe annealed by 40mbar HCF₂Cl partial pressure.

emission could be attributed to radiative recombination levels induced by impurities, like Cu, unintentionally incorporated during the CdTe deposition, or diffused from the front contact and buffer layers during the high temperature growth. The 1.47eV peak has been previously observed in polycrystalline CdTe (Cárdenas-García et al. 2005) and ascribed to the dislocation related Y-emission. In our untreated material, a clear dependence of this emission on the dislocations has not been demonstrated, but the disappearance of this peak in the annealed, high crystalline quality CdTe supports this attribution (Armani et al. 2007).

The HCF₂Cl annealing effect on the CdTe recombination mechanisms was studied by both CL spectroscopy and monochromatic (monoCL) mapping. CL spectra showed a drastic difference between untreated and HCF₂Cl annealed samples, as visible in Fig. 9. All the HCF₂Cl treated samples showed, in addition to the NBE emission, a broad CL band centered at 1.4eV which intensity increased by increasing the HCF₂Cl partial pressure, suggesting a strong dependence of this emission on the annealing. The literature studies on both single-crystal and polycrystalline CdTe (Consonni et al. 2006; Krustok et al. 1997) showed photoluminescence (PL) and CL bands centered at energies close to 1.4eV; their origin was attributed to a radiative recombination center like the well known A-center, due to a complex between a Cd vacancy (V_{Cd}) and a Cl impurity, in Cl-doped CdTe (Meyer et al. 1992; Stadler et al. 1995). The clear correlation between the 1.4eV band and the HCF₂Cl treatment supported the attribution of the 1.4eV band observed in our CdTe films to a complex like the A-centre. Either Cl or F impurities could be the origin of the level responsible for this transition. Several impurities, among which Cl and F, created acceptor levels with very similar energy values above the valence band edge as reported by Stadler et al. (Stadler W. et al. 1995). In particular the levels due to Cl and F differ solely by 9meV. The CL spectral resolution, lower than the PL one, did not allow determining the exact energy position of the 1.4 eV band with a precision better than 0.01eV. On this basis a clear attribution, to Cl or F, of the impurity creating the complex together to the V_{Cd} was impossible. The 1.4eV/NBE CL intensity ratios represented a tool to study the concentration of the V_{Cd} -Cl(F) complex responsible for the 1.4eV band; the comparison among the untreated and the annealed CdTe results obtained at 25keV have been summarized in Fig. 10.

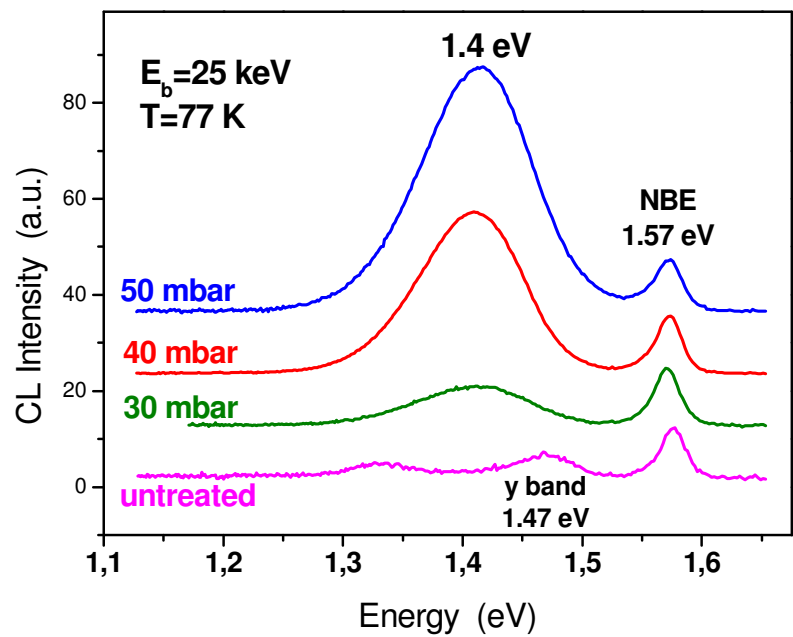


Fig. 9. Comparison among the low temperature (77 K) CL spectra ($E_b=25\text{keV}$) of untreated CdTe and samples annealed at a HCF_2Cl partial pressure of 30, 40 and 50 mbar.

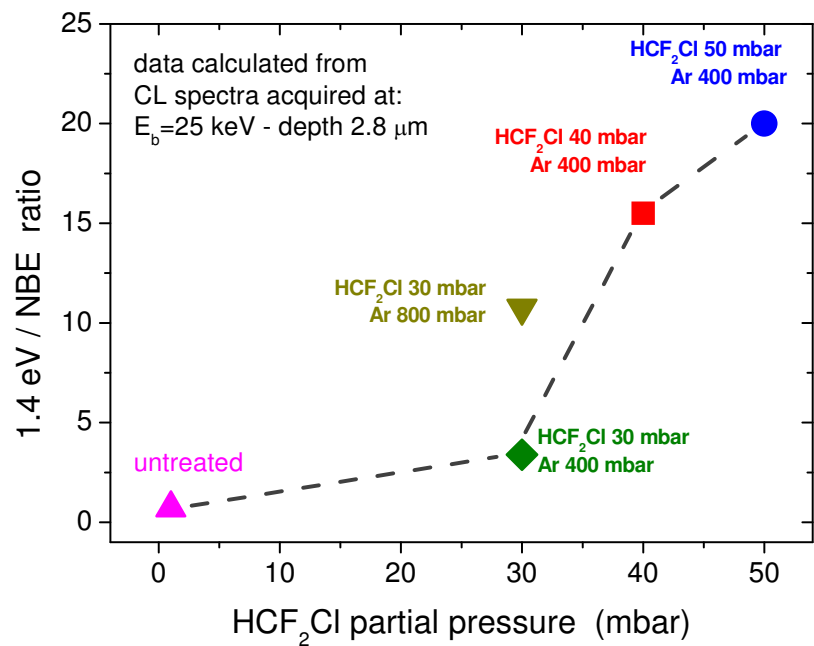


Fig. 10. Plot of the 1.4eV/NBE integrated intensity ratios. The experimental points have been calculated from spectra acquired in various regions of each CdTe film at $E_b= 25\text{keV}$.

One of the peculiarities of the CL technique is the possibility to increase the probing depth within the studied materials, by increasing E_b , by keeping the injection density in the generation volume constant. The effect of annealing on the CdTe luminescence behavior was expected to be more effective close to the CdTe surface. For this reason, CL spectra at lower beam energy ($E_b=12\text{keV}$), corresponding to a maximum penetration depth of 900nm below the CdTe surface, were collected. The comparison among untreated and annealed

samples showed a dependence of the 1.4 eV emission intensity on the HCF_2Cl partial pressure similar to the highly depth 25 keV analysis. A more detailed depth-resolved study of the $\text{V}_{\text{Cd-Cl}}(\text{F})$ complex distribution is performed by acquiring CL spectra at different E_B from 8 to 36 keV, corresponding to a probing depth between 0,36 and 4,6 μm . Fig. 11 showed the CL spectra, normalized to the NBE intensity, in order to better highlight the 1.4 eV band intensity variations. The 1.4 eV emission intensity decreased till the generation volume of the CL signal extended to about 2 μm , then kept almost constant for the following 2 μm . This behavior could be more clearly appreciated in the inset of the figure where the 1.4 eV/NBE integrated intensity ratio has been shown. Possible influence of material quality inhomogeneities along the deposition axis could be neglected because the NBE peak position did not change in the studied depth range as well as its intensity showed very small and random variations. The $\text{V}_{\text{Cd-Cl}}(\text{F})$ complex density was the highest close to the CdTe surface, due to the maximum effectiveness of the HCF_2Cl treatment however it decreased in depth, but not disappeared in the first 4 μm of the film.

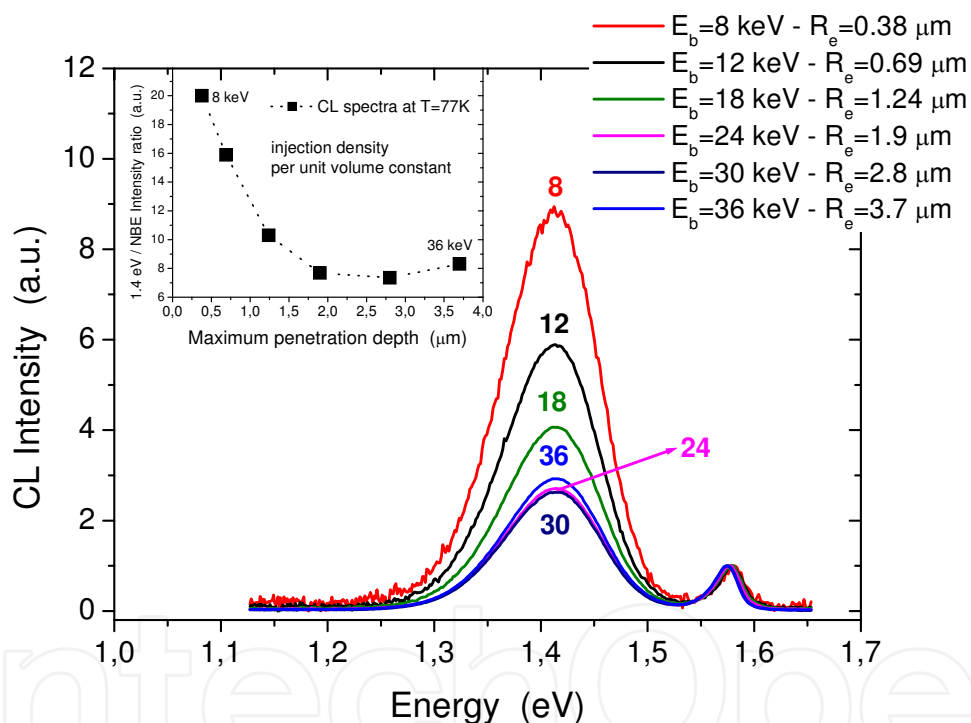


Fig. 11. Depth-dependent CL spectra acquired on the 40 mbar HCF_2Cl partial pressure annealed CdTe, by increasing E_b from 8 to 36 keV; in the inset the plot of the 1.4 eV/NBE integrated intensity ratios as a function of E_b has been shown.

The maximum E_B suitable for the SEM used for this work (36 keV) was not high enough to investigate the whole CdTe film, limiting the results to about a half of the material thickness. For this reason the samples were etched in order to eliminate a portion of CdTe, leaving the material near the CdTe/CdS interface free. After the etching procedure the decreasing thickness of CdTe film edge showed a slightly sloped surface extending from the upper surface of the front contact, down to about 1 μm above the CdTe/CdS interface. The SEM

image of the etched region has been shown in Fig. 13 a. CL analyses have been performed on the beveled CdTe surface, in the region closer to the interface, indicated as the “maximum etched surface” in Fig. 13 a. The comparison among the untreated CdTe and the annealed specimens was shown in Fig. 12. In the untreated and 30mbar treated samples, in addition to the NBE emission only the CL band centered at 1.47 eV has been observed. The 1.4eV band appeared only in cells treated with more than 30 mbar HCF_2Cl . By increasing the HCF_2Cl partial pressure, the 1.4eV CL intensity also increases confirming the behavior observed on the not-etched CdTe surface. On the other hand, when present, the 1.4eV CL intensities were lower than those observed on the not-etched surfaces and did not exceed the NBE intensity. This behavior was clear in Fig. 13 b, where the comparison among CL spectra acquired on the 40mbar HCF_2Cl etched surface at different depths approaching the CdTe/CdS interface was shown. The spectra were acquired from a small area (10 μm wide) in order to investigate regions at the same depth. The analyzed regions have been indicated by the colored squares in Fig. 13 a. The 1.4eV CL intensity decreased remarkably from the blue to the black curve, which corresponded to regions approaching the “maximum etched region”. Only in the spectrum acquired 3 μm far from this region the 1.4eV band was back the dominant one. The depth-dependent decrease of the 1.4eV CL intensity could be attributed to a not-uniform distribution of the $\text{V}_{\text{Cd-Cl}}(\text{F})$ complex responsible for that transition because of a low diffusion of the Cl (or F) atoms within the CdTe.

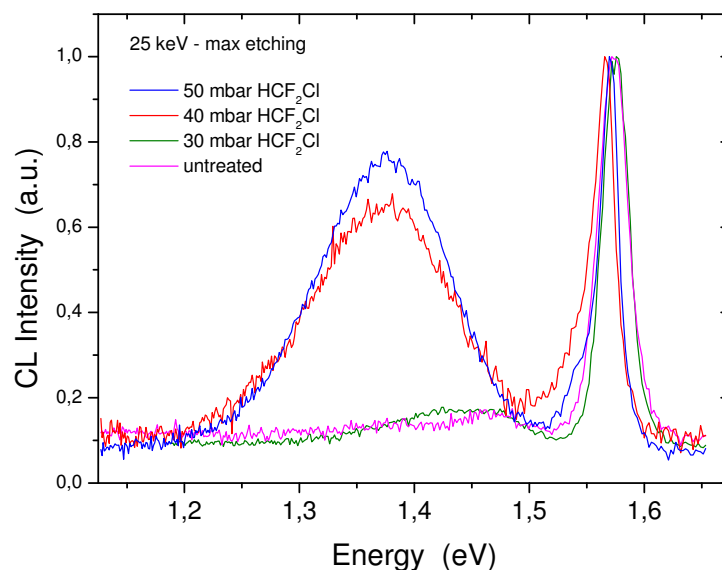


Fig. 12. Comparison among the low temperature (77 K) CL spectra ($E_B=25$ keV) of untreated CdTe and samples annealed at a HCF_2Cl partial pressure of 30, 40 and 50 mbar.

The spatial distribution of luminescence properties of CdTe was studied by acquiring monoCL images at the emission energies of the bands observed in the CL spectra, 1.57eV and 1.4eV respectively. The monoCL image collected at the NBE emission energy ($E=1.57\text{eV}$) showed the maximum intensity contribution from the central part of the grains (Fig. 14 b). The excitonic transitions came mainly from the CdTe grains, meaning that they were of good crystalline quality. On the other hand, in the same image the boundary regions between adjacent grains (*grain boundaries*) showed a dark contrast which corresponded to a very low radiative recombination efficiency. By acquiring the monoCL image at $E=1.4\text{eV}$

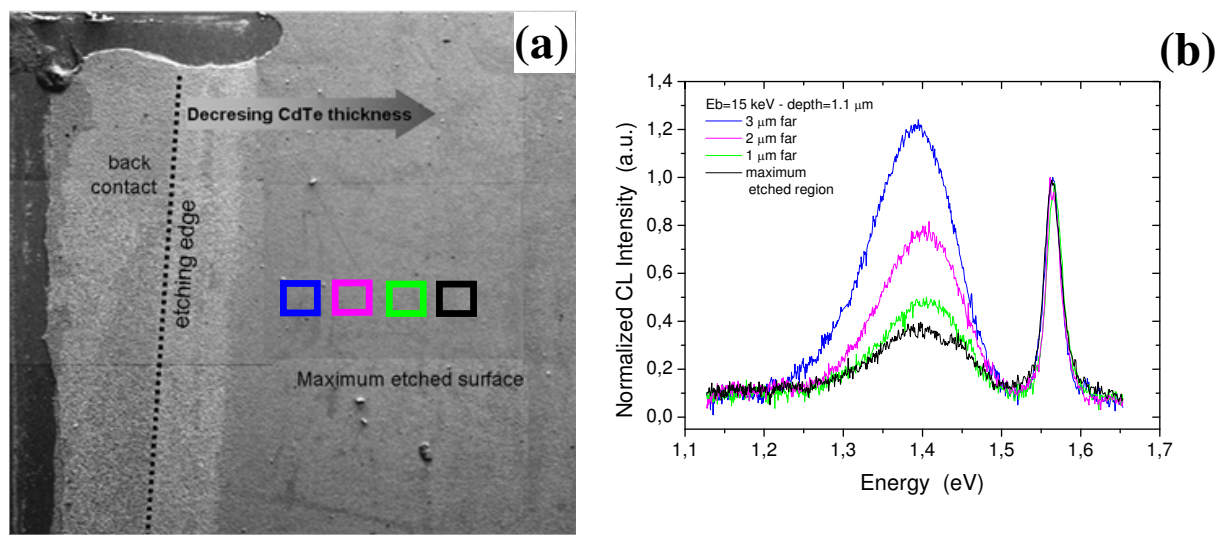


Fig. 13. a) SEM image of the etched surface of the solar cell annealed with 40 mbar HCF₂Cl partial pressure; b) comparison among the low temperature (77K) CL spectra ($E_b=15\text{keV}$) of the 40 mbar HCF₂Cl partial pressure etched solar cell.

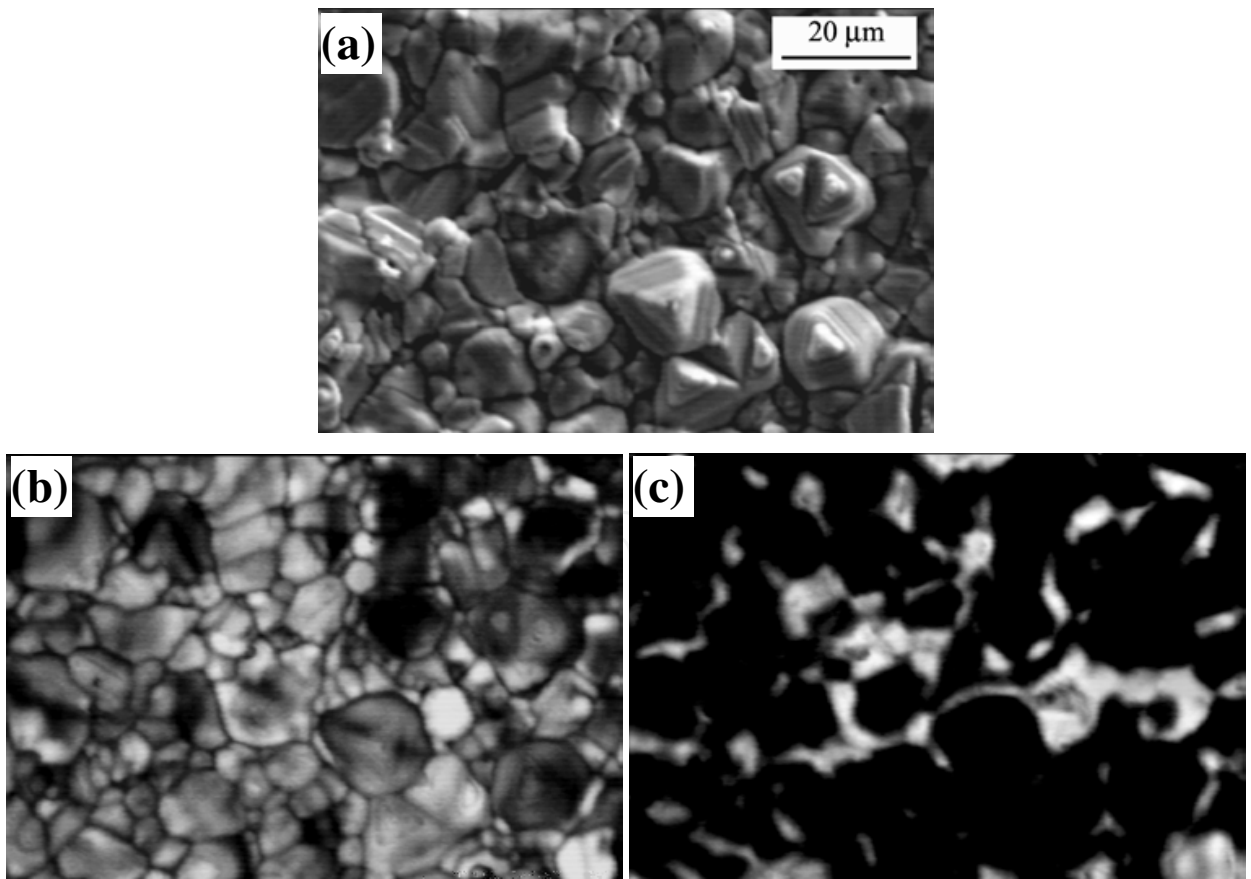


Fig. 14. 40 mbar HCF₂Cl partial pressure CdTe CL mapping; a) SEM image of the surface morphology; b) monoCL image at the NBE emission energy ($E=1.57\text{eV}$); c) monoCL at $E=1.4\text{eV}$ emission energy.

(Fig.14 c) a complementary CL intensity distribution has been observed. The bright contrast was concentrated in the grain boundaries. For a more clear representation of the correlation between surface morphology and CdTe radiative recombination properties the corresponding SEM image has been shown (Fig. 14 a).

Taking advantage on the possibility of focusing the SEM electron beam in suitable small regions, the spectroscopic behavior of the CL in a single grain has been studied. The adopted investigation conditions were in this case “fixed beam” at $E_B=12\text{keV}$, which corresponded to a sub-micrometric generation volume. The CL spectra acquired in the points marked by numbered colored circles on Fig. 15 a have been shown in Fig. 15 b. The curves were normalized to the NBE emission intensity. The spectra collected inside the CdTe grain numbered 2–5 showed a high-intensity NBE emission dominating the spectra. The 1.4eV band intensity, on the contrary, exceeded the NBE one in the spectra 1 and 6, collected close to the grain edges (*grain boundary*). The spatial distribution of the 1.4eV emission intensity could be directly correlated to the non homogenous density of the $V_{\text{Cd}}\text{-Cl(F)}$ complex responsible for that emission. A gettering of the native point defects (V_{Cd}), as well as of the incorporated impurities (Cl or F) could be suggested as the origin of this inhomogeneity. A preferential diffusion through the grain boundaries, of those impurities, during the high temperature annealing, has been supposed. The correlation between polycrystalline Cl doped CdTe structural properties and electronic levels created by the dopants in the CdTe gap has been discussed in the literature (Consonni et al. 2006, 2007) and the published results were in good agreement to those presented in this work.

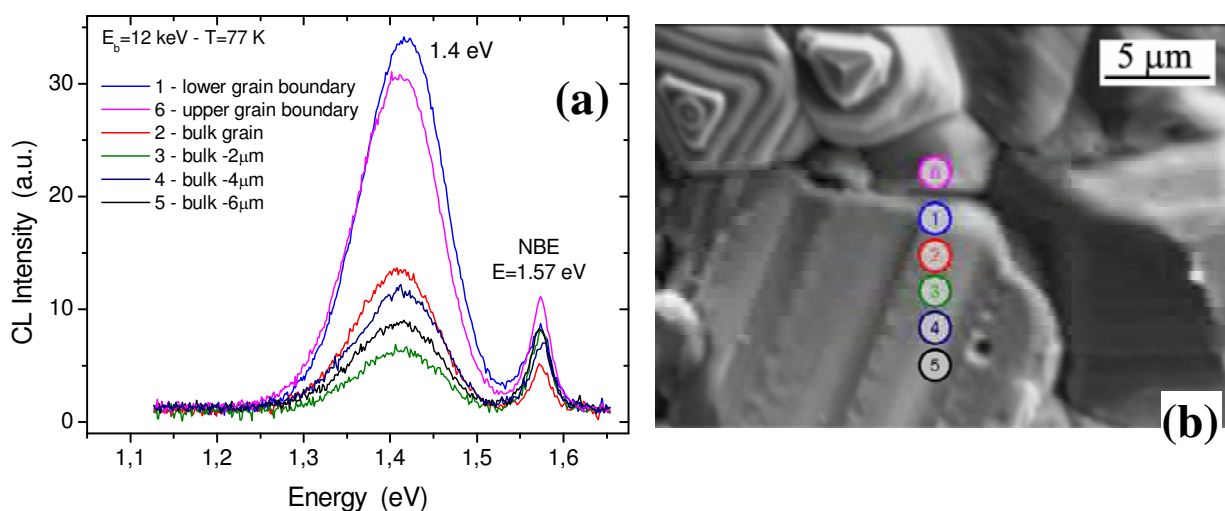


Fig. 15. a) Spatial variation of CL emissions, by acquiring the spectra in spot mode, in different points of a single CdTe grain; b) SEM image of the region where the CL spots are collected.

4.2 Comparison between the material properties and device performances

The behavior of the electro-optical properties of CdTe as a function of HCF_2Cl partial pressure, shown in the previous paragraph, did not allow to obtain information about the role of HCF_2Cl on the cell photovoltaics parameters and to investigate the transport processes taking place at the junction. The electrical properties of the annealed solar cells were compared to those of an untreated device. Dark reverse I-V curves were shown in Fig. 16 a, where the evolution of the reverse current (I_0) as a function of the HCF_2Cl partial pressure can be observed.

The diode ideality factor (A) has been calculated from those curves and its behavior as function of HCF_2Cl was also reported in Fig. 16 b. Specific processes occurring at the junction determined the reverse current and diode factor. In our case, it was observed a decrease of the reverse current when the HCF_2Cl partial pressure was increased. This behavior reached a minimum in the most efficient device obtained for this series, corresponding to 40mbar HCF_2Cl partial pressure ($J_{sc}=26.2\text{mA}/\text{cm}^2$, $V_{oc}=820\text{mV}$, $ff=0.69$, $\eta=14.8\%$, see Fig. 17). An increase of 10mbar more reactive gas in the annealing chamber yields to a degradation of the reverse current that was increased of various orders of magnitude, showing the high reactivity of the treatment and the impact of an excess annealing on the device electrical performance. At the same time, from the behavior of A , a variation of transport mechanism depending on the treatment conditions could be suggested (Fig. 16 b). For the untreated sample, $A=1.8$ indicated that recombination current dominated the junction transport mechanism or that high injection conditions were present. An increase of the HCF_2Cl partial pressure gave rise to a situation in which diffusion and recombination currents take place together until the case of 40mbar HCF_2Cl partial pressure was reached, where the minimum value of $A=1.2$, appointed to a predominant diffusion current. The cell treated with 50mbar of reactive gas partial pressure showed a sharp modification, by increasing again the diode factor n up to 1.8. The increase of the diode reverse saturation current was responsible for a drastic reduction of ff (Fig16 b), despite the J_{sc} and V_{oc} did not change appreciably from the others HCF_2Cl annealed devices.

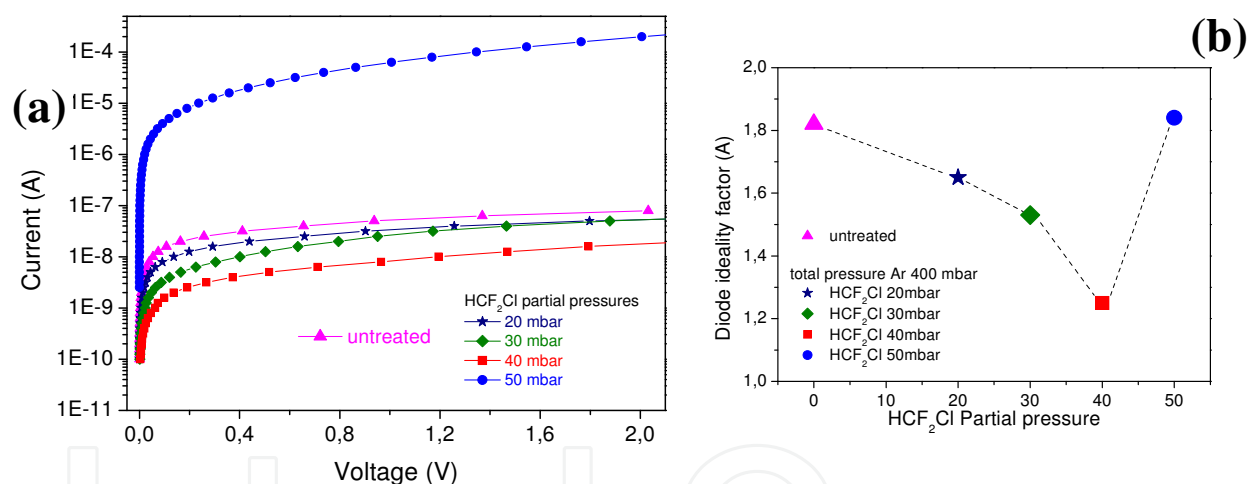


Fig. 16. a) Comparison among the dark reverse I-V curves for untreated and, 20, 30, 40 and 50 mbar of HCF_2Cl partial pressure treated solar cells; b) Diode ideality factor A as a function of the HCF_2Cl partial pressure.

The evolution of the J-V light curves (Fig. 17) of all samples showed an increase of the photovoltaic parameters by increasing the Freon partial pressure until 40mbar, while the J-V characteristic of the sample F50 showed a decrease of the fill factor to 0.25. The latter behavior could be related to a very strong intermixing between CdS and CdTe, due to the treatment, so that a very large p-n junction region was present.

A clear roll-over behavior of all the J-V curves was observed in the Fig. 17; mainly for the untreated sample and F20 and F50. This behavior was attributed to an n-p parasitic junction, opposite to the main p-n junction created by the back contact. We assume that this behavior was also strongly related to the incorporation of Cl impurities into CdTe. In our belief, the increment of the photocurrent collection should be essentially due to an increment of the

photogenerated minority carriers lifetime in the CdTe layer which suggested that the passivation of defects in absence of Cl contributed as non radiative recombination centers (Consonni et al. 2006). We considered the 50mbar HCF₂Cl cell an overtreated sample where the intermixing process was so strong that all the available CdS was consumed. The presence of shunt paths through the junction can explain the high reverse current and low fill factor values.

The luminescence properties observed on the CdTe material showed a continuous increase of the 1.4eV band intensity as a function of HCF₂Cl partial pressure; the device electrical characterization showed, on the contrary, a threshold at 40mbar partial pressure. Above this value the solar cell performances collapsed dramatically suggesting a critical correlation between HCF₂Cl annealing and junction properties.

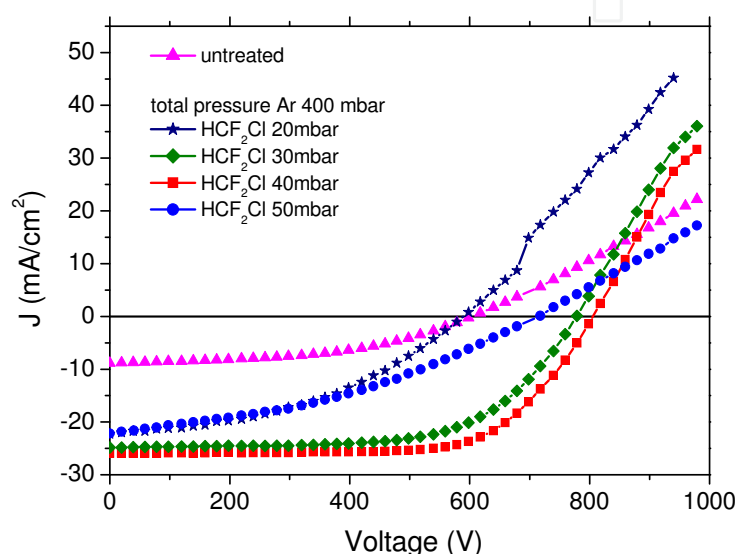


Fig. 17. Room temperature I-V characteristics under AM 1.5, 100mW/cm² illumination conditions of untreated solar cells compared to the 20, 30, 40 and 50 mbar HCF₂Cl partial pressures respectively.

The comparison between the diode factor A and the 1.4eV intensity behaviors suggested that the V_{Cd}-Cl(F) complex was beneficial for the device performances, but did not explain alone the maximum efficiency value measured for the 40 mbar annealed solar cells. A combined CdTe material doping and grain boundaries passivation effect had to be invoked. The absence of the 1.4eV band in the untreated and low HCF₂Cl partial pressure annealed CdTe after etching demonstrated that a non-radiative recombination centre was responsible for the low A values. This centre was then passivated by the Cl (or F) incorporation till the excess, for HCF₂Cl partial pressures above 40 mbar, deteriorated the p-n junction.

The complex V_{Cd}-Cl(F) formation could also be supported by the temperature dependent I-V analyses carried out on the CdTe thin film. The Arrhenius plot extracted from the CdTe dark conductivity as a function of the inverse of the temperature has been shown in Fig.18. The plot showed that, in the case of untreated CdTe the high calculated activation energy (324meV) has been related to a level due to the presence of occasional impurities like Cu, Ag or Au; the activation energy decreases by increasing the HCF₂Cl partial pressure, down to E_a=142meV for the material treated by 40mbar HCF₂Cl partial pressure. This value was in good agreement with those obtained in Cl (or F) doped CdTe single-crystals and attributed to the A-centre, due to the complex V_{Cd}-Cl(F) acceptor-like (Meyer et al. 1992).

A model of the effect of annealing as a function of HCF_2Cl partial pressure, on the bulk CdTe and its grain boundaries as well as on the CdTe-CdS intermixing mechanisms occurring at the interface has been showed in Fig. 19. The Cl (or F) impurities contained in the annealing gas penetrate into the material partially doping the CdTe. The major part was gettered to the grain boundaries, as observed in the monoCL image (Fig. 14 c), passivating them and improving conductivity. Contemporarily the interdiffusion of S in the CdTe and of Te in CdS has been promoted by creating an intermixing region, which thickness increased by increasing the HCF_2Cl partial pressure, pictured by the orange region between CdTe and CdS. The poor solar cell performances of the 50mbar HCF_2Cl partial pressure annealed device have been explained by a complete consumption of the CdS layer and by destruction of the main p-n junction.

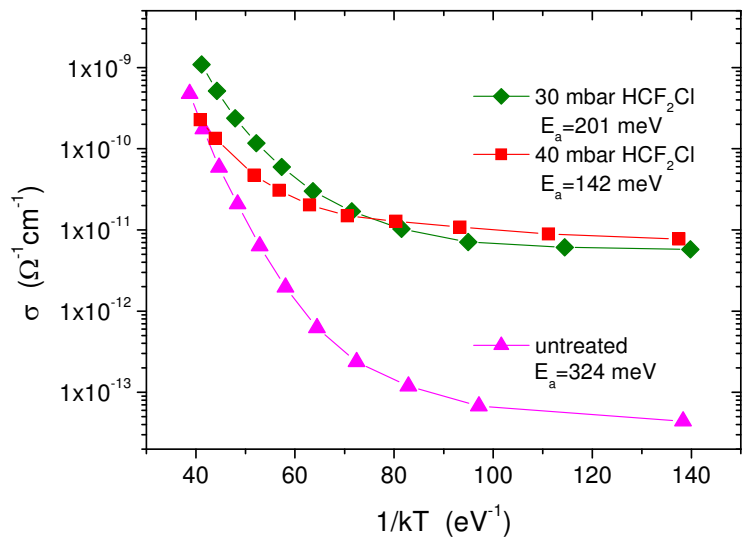


Fig. 18. Temperature dependent I-V curves collected from the untreated, 30mbar and 40mbar HCF_2Cl partial pressures respectively.

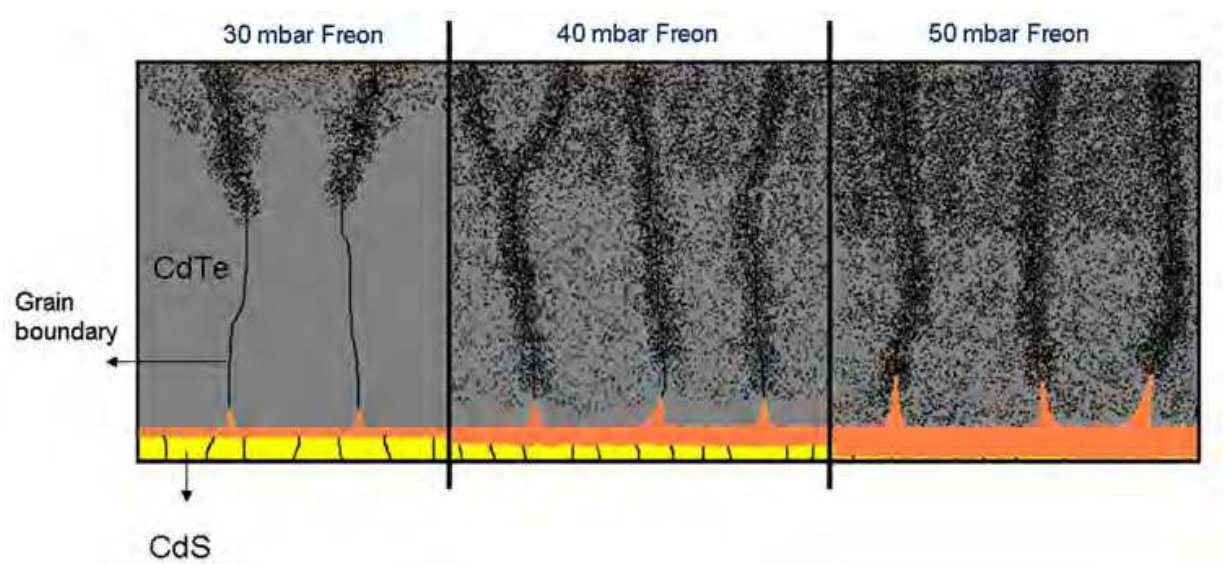


Fig. 19. Schematic representation of the effect of the HCF_2Cl treatment on defects distribution and intermixing junction formation

5. Conclusions

Thin films CdTe deposited by CSS have been submitted to a novel, full dry, post-deposition treatment based on HCF_2Cl gas. The annealing demonstrated to affect the structural properties of the materials through the loss of preferential orientation. Texture coefficient of the (111) Bragg reflection decreased from 2, for the untreated CdTe, down to 0.56 for the film treated with the highest HCF_2Cl partial pressure. On the contrary, the grain size did not show any change after annealing maintaining an average dimension of about $12\mu\text{m}$. These results were common for high temperature CSS deposited CdTe films, while a clear dependence on the HCF_2Cl partial pressure of the electro-optical properties of the films have been observed through the presence of a 1.4 eV CL band in the annealed specimens. The transition responsible for this emission involved an electronic level in the gap with an energy of about 0.15 eV above the valence band edge, which could be attributed to a complex between cadmium vacancy and an impurity probably identified in Cl or F ($\text{V}_{\text{Cd}}\text{-Cl/F}$) from the annealing gas.

The combined CL mapping and spectroscopy on single CdTe grains showed that the lateral distribution of this complex was not homogeneous in the grain, but it was concentrated close to the grain boundaries. The bulk grain, on the contrary, showed a high optical quality, evidenced by the predominance of the NBE emission. The in-depth effectiveness of the HCF_2Cl annealing has been demonstrated by correlating depth-dependent CL analyses to the study of the beveled CdTe surface due to the Br-methanol etching. High density of the $\text{V}_{\text{Cd}}\text{-Cl/F}$ complex responsible for the 1.4 eV band has been observed close to the CdTe surface; it decreased by increasing depth in the bulk region of the film about $5\mu\text{m}$ below the surface. By removing several microns of CdTe material and by approaching the CdTe/CdS interface, in the etched specimens, an HCF_2Cl partial pressure higher than 30 mbar was necessary to detect the 1.4 eV emission, this means to create the $\text{V}_{\text{Cd}}\text{-Cl/F}$ complex. On the other hand electrical characterization determined a threshold in the beneficial role of the HCF_2Cl annealing, showing the best solar cell performances for the 40 mbar partial pressure treated device. Temperature dependent I-V analyses showed a remarkable decrease of the electronic level activation energy, from 348meV to 142meV. The last value resulted in good agreement with the energy values of the A-center found in the literature.

The comparison between the diode factor A and the 1.4 eV CL band intensity behaviors evidenced that the $\text{V}_{\text{Cd}}\text{-Cl/F}$ complex was beneficial for the device performance, but does not explain alone the maximum efficiency value measured for the 40 mbar annealed solar cells. A tentative schematic model of the mechanisms occurring during post-deposition treatment, in the bulk CdTe and close to the CdTe/CdS interface have been also proposed. A combined CdTe-CdS intermixing and grain boundaries passivation effect has to be invoked.

6. References

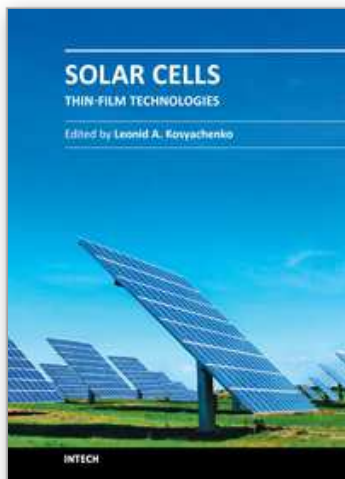
- Armani N., Salviati G., Nasi L., Bosio A., Mazzamuto S. and Romeo N., "Role of thermal treatment on the luminescence properties of CdTe thin films for photovoltaic applications", (2007) *Thin Solid Films*, vol. 515, pp. 6184-7, ISSN 00406090
- Barret C. and Massalski T.B. Structure of Metals, edited by Pergamon, Oxford, p. 204 (1980)
- Barrioz, V.; Lamb, D.A.; Jones, E.W. & Irvine, S.J.C. (2010). Suitability of atmospheric-pressure MOCVD CdTe solar cells for inline production scale. *Materials Research Society Symposium Proceedings*; ISBN: 978-160511138-4; San Francisco, CA; April 2009

- Bätzner, D.L.; Romeo, A.; Zogg, H.; Wendt, R. & Tiwari, A.N. (2001) Development of efficient and stable back contacts on CdTe/CdS solar cells. *Thin Solid Films*, Vol.387, No.1-2, May 2001, pp. 151-154. ISSN: 00406090.
- Birkmire, R.W.; Meyers, P.V. (1994) Processing issues for thin-film CdTe cells and modules, *Proceedings of the 24th IEEE Photovoltaic Specialists Conference*, ISSN: 01608371, Waikoloa, HI, USA, December 1994.
- Bosio, A.; Romeo, N.; Mazzamuto, S. and Canevari V. (2006), Polycrystalline CdTe thin films for photovoltaic applications. *Progress in Crystal Growth and Characterization of Materials*, Vol.52, No.4, December 2006, pp. 247-279, ISSN: 09608974.
- Aguilar-Hernandez J, Sastre-Hernandez J, Mendoza-Perez R, Cardenas-Garcia M and Contreras-Puente G (2005), "Influence of the CdCl₂ thermal annealing on the luminescent properties of CdS-CSVT thin films", *Physica Status Solidi C - Conference and Critical Reviews*, vol. 2, No 10, p.p. 3710-3713, ISSN: 1610-1634
- Chu, T.L.; Chu, S.S.; Ferekides, C.; Wu, C.Q.; Britt, J. & Wang, C. (1991). 13.4% efficient thin-film CdS/CdTe solar cells. *Journal of Applied Physics*, Vol.70, No.12, 1991, pp. 7608-7612. ISSN: 00218979
- Compaan, A.D.; Tabor, C.N.; Li, Y.; Feng, Z. & Fischer, A. (1993). CdS/CdTe Solar cells by RF sputtering and by laser physical vapor deposition. *Proceedings of the 23rd IEEE Photovoltaic Specialists Conference*, pp. 394-399, ISBN: 0780312201, Louisville, KY, USA; May 10-14, 1993
- Consonni V., Feuillet G. and Renet S., (2006), "Spectroscopic analysis of defects in chlorine doped polycrystalline CdTe" *J. Appl. Phys.*, vol. 99, p.p. 053502-1/7, ISSN: 0021-8979
- Consonni V., Feuillet G., Bleuse j. and Donatini F., (2007) "Effects of island coalescence on the compensation mechanisms in chlorine doped polycrystalline CdTe", *J. Appl. Phys.*, vol. 101, p.p- 063522-1/6, ISSN: 0021-8979
- Cruz, L.R.; Kazmerski, L.L.; Moutinho, H.R.; Hasoon, F.; Dhere, R.G. & De Avelaz, R. (1999). Influence of post-deposition treatment on the physical properties of CdTe films deposited by stacked elemental layer processing. *Thin Solid Films*, Vol.350, No. 1, August 1999, pp. 44-48. ISSN: 00406090
- Cunningham, D.; Davies, K.; Grammond, L.; Mopas, E.; O'Connor, M.; Rubcich, M; Sadeghi, M.; Skinner, D. and Trumbly, T. (2000). Large area Apollo module performance and reliability. *Proceedings of the 28th IEEE Photovoltaic Specialists Conference*.
- Enriquez, J.P. and Mathew, X. (2004). XRD study of the grain growth in CdTe films annealed at different temperatures. *Solar Energy Materials and Solar Cells*. Vol. 81, No. 3, February 2004, pp. 363-369, ISSN: 09270248
- Ferekides, C.S.; Marinsky, D.; Viswanathan, V.; Tetali, B.; Palekis, V.; Selvaraj, P. & Morel, D.L. (2000). High efficiency CSS CdTe solar cells. *Thin Solid Films*. Vol.361, (February 2000), pp. 520-526, ISSN: 00406090
- Grillo V., Armani N., Rossi F., Salviati G. and Yamamoto N., (2003), "A.L.E.S.: A random walk simulation approach to cathodoluminescence processes in semiconductors" *Inst. Phys. Conf. Ser.* No 180, p.p. 559-562, ISSN 0951-3248
- Hartley, A.; Irvine, S.J.C.; Halliday, D.P. & Potter, M.D.G. (2001). The influence of CdTe growth ambient on MOCVD grown CdS/CdTe photovoltaic cells. *Thin Solid Films*. Vol.387, No.1-2, May 2001, pp. 89-91. ISSN: 00406090
- Hernández-Contreras, H.; Contreras-Puente, G. , Aguilar-Hernández, J. , Morales-Acevedo, A. , Vidal-Larramendi, J. & Vigil-Galán, O. (2002). CdS and CdTe large area thin films processed by radio-frequency planar-magnetron sputtering. *Thin Solid Films*. Vol.403-404, February 2002, Pages 148-152. ISSN: 00406090

- Josell, D.; Beauchamp, C. R.; Jung, S.; Hamadani, B. H.; Motayed, A.; Richter, L. J.; Williams, M.; Bonevich, J. E.; Shapiro, A.; Zhitenev, N. & Moffat, T. P. (2009). Three Dimensionally Structured CdTe Thin-Film Photovoltaic Devices with Self-Aligned Back-Contacts: Electrodeposition on Interdigitated Electrodes. *Journal of Electrochemical Society*. Vol.156, No.8, (June 2009). pp. H654-H660, ISSN: 0013-4651
- Kosyachenko, L.A.; Mathew, X.; Motushchuk, V.V. & Sklyarchuk, V.M. (2006). Electrical properties of electrodeposited CdTe photovoltaic devices on metallic substrates: study using small area Au-CdTe contacts. *Solar Energy*. Vol.80, No.2, (February 2006), pp. 148-155, ISSN: 0038092X
- Krustok, J; Madasson, J; Hjelt, K, and Collan H (1997) "1.4 eV photoluminescence in chlorine-doped polycrystalline CdTe with a high density of defects" *Journal of Materials Science*, vol. 32 No: 6 p.p. 1545-1550, ISSN 00222461
- Lane, D.W.; Rogers, K.D.; Painter, J.D.; Wood, D.A. & Ozsan, M.E. (2000). Structural dynamics in CdS-CdTe thin films. *Thin Solid Films*, Vol.361, February 2000, pp. 1-8. ISSN: 00406090
- Levy-Clement, C. (2008). Thin film electrochemical deposition at temperatures up to 180 °C for photovoltaic applications. *Proceedings of Interfacial Electrochemistry and Chemistry in High Temperature Media - 212th ECS Meeting*; ISBN: 978-160560312-4; Washington, DC; October 2007
- Lincot, D. (2005). Electrodeposition of chalcogenide semiconductors. *Proceedings of 207th Electrochemical Society Meeting*, Quebec, May 2005.
- Luschitz, J.; Siepchen, B.; Schaffner, J.; Lakus-Wollny, K.; Haindl, G.; Klein, A. and Jaegermann, W. (2009) CdTe thin film solar cells: Interrelation of nucleation, structure, and performance. *Thin Solid Films*, Vol. 517, No.7, February 2009, pp. 2125-2131, ISSN: 00406090.
- McCandless, B.E. & Birkmire, R.W. (1991) Analysis of post deposition processing for CdTe/CdS thin film solar cells. *Solar Cells*, vol. 31, No. 6, December 1991, pp. 527-535, ISSN: 03796787.
- McCandless, B.E.; Moulton, L.V. and Birkmire, R.W. (1997). Recrystallization and sulfur diffusion in CdCl₂-treated CdTe/CdS thin films. *Progress in Photovoltaics: Research and Applications*, Vol. 5, No.4, July 1997, pp. 249-260, ISSN: 10627995.
- McCandless, B.E. (2001). Thermochemical and kinetic aspects of cadmium telluride solar cell processing. *MRS Proceedings*, Vol.668, H1.6, ISSN: 02729172, San Francisco, CA, USA; April 16-20, 2001
- McCandless, B.E. & Sites, J.R. (2003) Cadmium telluride solar cells in: *Handbook of Photovoltaic Science and Engineering* Luque, A. and Hegedus, S.S., pp. 617-662, John Wiley & Sons Ltd, ISBN: 9780471491965, Chichester, UK.
- McCandless, B.E. and Dobson, K.D. (2004). Processing options for CdTe thin film solar cells. *Solar Energy*, Vol. 77, No.6, December 2004, pp. 839-856, ISSN: 0038092X.
- Merano, M.; Sonderegger, S.; Crottini, A.; Collin, S.; Pelucchi, E.; Renucci, P.; Malko, A.; Baier, M.H.; Kapon, E.; Ganiere, J.D. and Deveaud, B. (2006) Time-resolved cathodoluminescence of InGaAs/AlGaAs tetrahedral pyramidal quantum structures. *Applied Physics B: Lasers and Optics*, Vol. 84, No.1-2, July 2006, pp. 343-350, ISSN: 09462171.
- Meyer BK, Stadler W, Hofmann DM, Ömling P, Sinerius D and Benz KW (1992), On the Nature of the Deep 1.4 eV Emission Bands in CdTe - a Study with Photoluminescence and ODMR Spectroscopy, *Journal of Crystal Growth*, vol. 117, No 1-4, p.p. 656-659 ISSN: 0022-0248

- Moutinho, H.R.; Al-Jassim, M.M.; Levi, D.H.; Dippo, P.C. and Kazmerski, L.L. (1998). Effects of CdCl₂ treatment on the recrystallization and electro-optical properties of CdTe thin films. *Journal of Vacuum Science and Technology A: Vacuum, Surfaces and Films*. Vol.16, No.3, May 1998, pp. 1251-1257, ISSN: 07342101.
- Moutinho, H.R.; Dhere, R.G.; Al-Jassim, M.M.; Levi D.H. and Kazmerski L.L. (1999). Investigation of induced recrystallization and stress in close-spaced sublimated and radio-frequency magnetron sputtered CdTe thin films. *Journal of Vacuum Science and Technology A: Vacuum, Surfaces and Films*. Vol.17, No.4, 1999, pp. 1793-1798, ISSN: 07342101.
- Paulson P.D. and Dutta V (2000). Study of in situ CdCl₂ treatment on CSS deposited CdTe films and CdS/CdTe solar cells, *Thin Solid Films*, vol. 370, p.p. 299-306, ISSN 00406090
- Perrenaud, J, Kranz, L; Buecheler S.; Pianezzi, F. and Tiwari, A.N. (2011). The use of aluminium doped ZnO as transparent conductive oxide for CdS/CdTe solar cells. *Thin Solid Films*. Article in Press. ISSN: 00406090
- Plotnikov, V., Liu, X., Paudel, N., Kwon, D., Wieland & K.A., Compaan, A.D. (2011). Thin-film CdTe cells: Reducing the CdTe. *Thin Solid Films*. Article in Press. ISSN: 00406090
- Potlog, T.; Khrypunov, G.; Kaelin, M.; Zogg, H. & Tiwari, A.N. (2007). Characterization of CdS/CdTe solar cells fabricated by different processes. *Materials Research Society Symposium Proceedings*, ISBN: 978-155899972-5, San Francisco, CA; April 2007
- Potter, M.D.G.; Halliday, D.P.; Cousins, M. & Durose, K. (2000). Study of the effects of varying cadmium chloride treatment on the luminescent properties of CdTe/CdS thin film solar cells. *Thin Solid Films*, Vol.361, February 2000, pp. 248-252. ISSN: 00406090
- Romeo, A.; Bätzner, D.L.; Zogg, H. & Tiwari, A.N. (2000). Recrystallization in CdTe/CdS. *Thin Solid Films*. Vol.361 (February 2000), pp. 420-425, ISSN: 00406090
- Romeo, A.; Buecheler, S.; Giarola, M.; Mariotto, G.; Tiwari, A.N.; Romeo, N.; Bosio, A. & Mazzamuto, S. (2009). Study of CSS- and HVE-CdTe by different recrystallization processes. *Thin Solid Films*, Vol.517, No.7, February 2009, pp. 2132-2135. ISSN: 00406090
- Romeo, N.; Bosio, A.; Tedeschi, R.; Romeo, A. & Canevari, V. (1999). Highly efficient and stable CdTe/CdS thin film solar cell. *Solar Energy Materials and Solar Cells*, Vol.58, No.2, June 1999, pp.209-218. ISSN: 09270248
- Romeo, N.; Bosio, A.; Canevari, V. & Podestà, A. (2004). Recent progress on CdTe/CdS thin film solar cells. *Solar Energy*, Vol.77, No.6, December 2004, pp. 795-801. ISSN: 0038092X
- Romeo, N.; Bosio, A.; Mazzamuto, S.; Podestà, A. and Canevari, V. (2005). The Role of Single Layers in the Performance of CdTe/CdS thin film solar cells. *Proceedings of 25th Photovoltaic Energy Conference and Exhibition*, Barcelona, Spain, June 2005.
- Romeo, N.; Bosio, A.; Romeo, A.; Mazzamuto, S. & Canevari, V. (2006). High Efficiency CdTe/CdS Thin Film Solar Cells Prepared by Treating CdTe Films with a Freon Gas in Substitution of CdCl₂. *Proceedings of the 21st European Photovoltaic Solar Energy Conference and Exhibition*, pp.1857-1860, ISBN 3-936338-20-5, Dresden, Germany, September 4-8, 2006.
- Romeo, N.; Bosio, A.; Mazzamuto, S.; Romeo, A. & Vaillant-Roca, L. (2007). "High efficiency cdte/cds thin film solar cells with a novel back-contact", *Proceedings of the 22nd European Photovoltaic Solar Energy Conference and Exhibition*, pp. 1919-1921, Milan; Italy.

- Romeo, N.; Bosio, A.; Romeo, A. & Mazzamuto, S. (2010). A CdTe thin film module factory with a novel process. *Proceedings of 2009 MRS Spring Meeting*; Vol.1165, pp. 263-273, ISBN: 978-160511138-4, San Francisco, CA, USA; April 13-17, 2009
- Schulz, D.L.; Pehnt, M.; Rose, D.H.; Urgiles, E.; Cahill, A.F.; Niles, D.W.; Jones, K.M.; Ellingson, R.J.; Curtis, C.J.; Ginley, D.S. (1997). CdTe Thin Films from Nanoparticle Precursors by Spray Deposition. *Chemistry of Materials*. Vol.9. No.4, April 1997, pp. 889-900. ISSN: 08974756
- Stadler, W.; Hoffmann, D.M.; Alt, H.C.; Muschik, T.; Meyer, B.K.; Weigel, E.; Müller-Vogt, G.; Salk, M.; Rupp, E. and Benz, K.W. (1995) Optical investigations of defects in $\text{Cd}_{1-x}\text{Zn}_x\text{Te}$, *Physical Review B*, vol.51, No.16 1995, pp. 10619-10630, ISSN: 01631829.
- Sze, S. (1981). *Physics of Semiconductor Devices* (2nd ed.), Wiley, ISBN:9780471143239, New York.
- Yacobi, B.G. & Holt, D.B. (1990) *Cathodoluminescence microscopy of inorganic solids*, Plenum Press, ISBN: 0306433141, New York and London.
- Yi, X. & Liou, J.J. (1995). Surface oxidation of polycrystalline cadmium telluride thin films for Schottky barrier junction solar cells. *Solid-State Electronics*. Vol.38, No.6, (1995), pp.1151-1154, ISSN: 00381101.
- Yoshida, T. (1992). Analysis of photocurrent in screen-printed CdS/CdTe solar cells. *Journal of the Electrochemical Society*. Vol.139, No.8, August 1992, pp. 2353-2357. ISSN: 00134651
- Yoshida, T. (1995). Photovoltaic properties of screen-printed CdTe/CdS solar cells on indium-tin-oxide coated glass substrates. *Journal of the Electrochemical Society*. Vol.142, No.9, September 1995, pp. 3232-3237. ISSN: 00134651
- Wu, X.; Keane, J.C.; Dhere, R.G.; DeHart, C.; Duda, A.; Gessert, T.A.; Asher, S.; Levi, D.H. and Sheldon, P. (2001 a). 16.5% efficient CdS/CdTe polycrystalline thin-film solar cell, *Proceedings of the 17th E-PVSEC*, München, Germany; October 2001.
- Wu, X.; Asher, S.; Levi, D.H.; King, D.E.; Yan, Y.; Gessert, T.A. & Sheldon, P. (2001 b). Interdiffusion of CdS and Zn_2SnO_4 layers and its application in CdS/CdTe polycrystalline thin-film solar cells. *Journal of Applied Physics*, Vol.89, No.8, April 2001, pp. 4564-4569. ISSN: 00218979
- Wu, X. (2004). High-efficiency polycrystalline CdTe thin-film solar cells. *Solar Energy*. Vol.77, No.6, (December 2004), pp. 803-814, ISSN: 0038092X
- Wu, X.; Zhou, J.; Duda, A.; Yan, Y.; Teeter, G.; Asher, S.; Metzger, W.K.; Demtsu, S.; Wei, S.-Huai. & Noufi, R. (2007). Phase control of Cu_xTe film and its effects on CdS/CdTe solar cell. *Thin Solid Films*, Vol.515, No.15 SPEC. ISS., May 2007, pp. 5798-5803, ISSN: 00406090
- Xiaonan Li., Niles D. W., Hasoon F. S., Matson R. J, and Sheldon P. (1999). Effect of nitric-phosphoric acid etches on material properties and back-contact formation of CdTe-based solar cells. *J. Vac. Sci. Technol. A*, vol. 17, No 3, p.p. 805-809 ISSN: 07342101.
- Zanio, K.; Willardson R.K. & Beer, A.C. (1978). *Cadmium telluride. Volume 13 of Semiconductors and semimetals*. Cadmium telluride, Academic Press, ISBN 0127521135, 9780127521138, London, UK
- Zhou, J.; Wu, X.; Duda, A.; Teeter, G. & Demtsu, S.H. (2007). The formation of different phases of Cu_xTe and their effects on CdTe/CdS solar cells. *Thin Solid Films*, Vol. 515, No.18, June 2007, pp. 7364-7369, ISSN: 00406090
- Zoppi, G.; Durose, K.; Irvine, S.J.C. & Barrioz, V. (2006). Grain and crystal texture properties of absorber layers in MOCVD-grown CdTe/CdS solar cells. *Semiconductor Science and Technology*. Vol.21, No.6, June 2006, pp. 763-770. ISSN: 02681242



Solar Cells - Thin-Film Technologies

Edited by Prof. Leonid A. Kosyachenko

ISBN 978-953-307-570-9

Hard cover, 456 pages

Publisher InTech

Published online 02, November, 2011

Published in print edition November, 2011

The first book of this four-volume edition is dedicated to one of the most promising areas of photovoltaics, which has already reached a large-scale production of the second-generation thin-film solar modules and has resulted in building the powerful solar plants in several countries around the world. Thin-film technologies using direct-gap semiconductors such as CIGS and CdTe offer the lowest manufacturing costs and are becoming more prevalent in the industry allowing to improve manufacturability of the production at significantly larger scales than for wafer or ribbon Si modules. It is only a matter of time before thin films like CIGS and CdTe will replace wafer-based silicon solar cells as the dominant photovoltaic technology. Photoelectric efficiency of thin-film solar modules is still far from the theoretical limit. The scientific and technological problems of increasing this key parameter of the solar cell are discussed in several chapters of this volume.

How to reference

In order to correctly reference this scholarly work, feel free to copy and paste the following:

Nicola Armani, Samantha Mazzamuto and Lidice Vaillant-Roca (2011). Influence of Post-Deposition Thermal Treatment on the Opto-Electronic Properties of Materials for CdTe/CdS Solar Cells, Solar Cells - Thin-Film Technologies, Prof. Leonid A. Kosyachenko (Ed.), ISBN: 978-953-307-570-9, InTech, Available from: <http://www.intechopen.com/books/solar-cells-thin-film-technologies/influence-of-post-deposition-thermal-treatment-on-the-opto-electronic-properties-of-materials-for-cd>

INTECH
open science | open minds

InTech Europe

University Campus STeP Ri
Slavka Krautzeka 83/A
51000 Rijeka, Croatia
Phone: +385 (51) 770 447
Fax: +385 (51) 686 166
www.intechopen.com

InTech China

Unit 405, Office Block, Hotel Equatorial Shanghai
No.65, Yan An Road (West), Shanghai, 200040, China
中国上海市延安西路65号上海国际贵都大饭店办公楼405单元
Phone: +86-21-62489820
Fax: +86-21-62489821

© 2011 The Author(s). Licensee IntechOpen. This is an open access article distributed under the terms of the [Creative Commons Attribution 3.0 License](https://creativecommons.org/licenses/by/3.0/), which permits unrestricted use, distribution, and reproduction in any medium, provided the original work is properly cited.

IntechOpen

IntechOpen